

Quasi-Bayesian Local Projections: Simultaneous Inference and Extension to the Instrumental Variable Method

Masahiro Tanaka*

March 27, 2025

Abstract

While local projections (LPs) are widely used for impulse response analysis, existing Bayesian approaches face fundamental challenges because a set of LPs does not constitute a likelihood function. Prior studies address this issue by constructing a pseudo-likelihood, either by treating LPs as a system of seemingly unrelated regressions with a multivariate normal error structure or by applying a quasi-Bayesian approach with a sandwich estimator. However, these methods lead to posterior distributions that are not “well calibrated,” preventing proper Bayesian belief updates and complicating the interpretation of posterior distributions. To resolve these issues, we propose a novel quasi-Bayesian approach for inferring LPs using the Laplace-type estimator. Specifically, we construct a quasi-likelihood based on a generalized method of moments criterion, which avoids restrictive distributional assumptions and provides well-calibrated inferences. The proposed framework enables the estimation of simultaneous credible bands and naturally extends to LPs with an instrumental variable, offering the first Bayesian treatment of this method. Furthermore, we introduce two posterior simulators capable of handling the high-dimensional parameter space of LPs with the Laplace-type estimator. We demonstrate the effectiveness of our approach through extensive Monte Carlo simulations and an empirical application to U.S. monetary policy.

Keywords: local projections; Bayesian inference; Laplace-type estimator; instrumental variable method; generalized method of moments

1 Introduction

Local projections (LPs) (Jordà, 2005) are a set of equations that relate an outcome variable measured at different time periods to exogenous variables. LPs are primarily used for impulse response analysis in which a sequence of coefficients of an exogenous shock across LPs represents an impulse response function (IRF).¹

While the frequentist inference of LPs has been extensively researched, studies on the Bayesian approach to LPs are scarce (Tanaka, 2020a; Ferreira et al., forthcoming). The Bayesian inference

*Faculty of Economics, Fukuoka University, Fukuoka, Japan. Address: 8-19-1, Nanakuma, Jonan, Fukuoka, Japan 814-0180. E-mail: gspddlnt45@toki.waseda.jp.

¹See Jordà (2023); Jordà and Taylor (2024) for a review of LPs.

of LPs is not a trivial task because a set of LPs does not constitute a probabilistic model of the underlying data-generating process (DGP), implying that LPs do not form a likelihood function. Previous studies have addressed this issue using a pseudo-likelihood approach. Tanaka (2020a) treats a set of LPs as a system of seemingly unrelated regressions (Zellner, 1962), assuming that the error terms of LPs are distributed according to a multivariate normal distribution, thereby obtaining the pseudo-likelihood in a standard form.² Posterior draws are then simulated using a standard Gibbs sampler and the resulting draws are used for posterior analysis. Tanaka (2020b) analytically derives the likelihood under the assumption that the DGP is a stationary vector moving average process, demonstrating that the covariance matrix of LPs is a function of a subset of the coefficients and covariance matrix of structural innovations. This result suggests that the misspecification in the pseudo-likelihood lies in treating the covariance matrix of the error terms as an independent parameter. However, although the Monte Carlo simulations presented by Tanaka (2020b) suggest that the coefficients and covariance matrix are consistently estimated, the misspecified posterior cannot be interpreted straightforwardly (Walker, 2013). Indeed, the coverage probability of the credible interval based on the pseudo-posterior can deviate significantly from the nominal level, as shown in the simulation study presented later in this paper.

Ferreira et al. (forthcoming) propose a quasi-Bayesian approach. Like Tanaka (2020a), they simulate posterior draws based on the pseudo-likelihood but estimate the posterior variance of the coefficients using Müller’s (2013) sandwich estimator, applied equation by equation. This approach relies on asymptotic theory and uses only a point estimate to compute the posterior variance. Ferreira et al. (forthcoming) justify their method on the grounds that “the misspecification in the likelihood arises from the assumption around the innovations” and “the estimator has to be thought of as the Quasi-Maximum Likelihood estimator of a pseudo-true parameter” (Section 2.1 of Ferreira et al., forthcoming).

Despite their considerable strengths, we identify two major issues with these existing approaches. First, in both Tanaka (2020a) and Ferreira et al. (forthcoming), posterior inference cannot be interpreted as a proper belief update, as the pseudo-likelihood is not “well calibrated.” In particular, the approach of Ferreira et al. (forthcoming), which relies on asymptotic theory, is not as valid in finite samples as it is in large samples (i.e., when the prior’s influence on the posterior has diminished). Specifically, the point estimate in finite samples may inadequately capture the effects of prior information on the posterior. Second, Ferreira et al.’s (forthcoming) approach cannot provide simultaneous credible bands (Jordà, 2009; Montiel Olea and Plagborg-Møller, 2019), as it estimates the posterior covariances separately for each LP. Since inference on an IRF constitutes a multiple testing problem, estimating a simultaneous credible band is a crucial component of impulse response analysis.

To address these issues, this study proposes a quasi-Bayesian approach to LPs using the Laplace-type estimator (LTE) (Kim, 2002; Chernozhukov and Hong, 2003). In this framework, the coefficients are inferred from a set of moment conditions and the quasi-likelihood is constructed using a generalized method of moments (GMM) criterion (Hansen, 1982). This approach eliminates the need to impose stringent distributional assumptions on error terms or explicitly estimate their covariance matrix. Furthermore, the GMM-based approach can be readily extended to the instrumental variable (IV) setting, referred to as LPs with an IV (LP-IV) (Ramey, 2016; Stock and Watson, 2018).

The proposed approach has three key advantages over existing methods. First, the quasi-posterior based on the LTE is “well calibrated” in that the credible intervals estimated directly

²Huber et al. (2024) use the same approach. In the frequentist setting, El-Shagi (2019) also treats LPs as seemingly unrelated regressions and estimates them using the feasible generalized least squares estimator.

from the generated draws closely align with their asymptotic counterparts. This suggests that the LTE effectively manages the relative contributions of the likelihood and prior components to the posterior. Second, the proposed approach enables the estimation of simultaneous credible bands using the method introduced by Montiel Olea and Plagborg-Møller (2019). Third, it naturally accommodates IV estimation. While the frequentist literature includes methodological contributions (Ramey, 2016; Stock and Watson, 2018; Plagborg-Møller and Wolf, 2021, 2022) and empirical applications (Jordà et al., 2015; Ramey and Zubairy, 2018; Mertens and Montiel Olea, 2018; Jordà et al., 2020), to the best of the author’s knowledge, this is the first to propose a feasible Bayesian approach to LP-IV.³

Another major contribution of this study is the development of practical posterior simulators. While the idea of applying the LTE to LPs is conceptually straightforward, it has been unexplored, likely due to the computational challenges associated with posterior simulation. One significant difficulty stems from the high dimensionality of the sampling space, as a set of LPs can involve hundreds or even thousands of unknown parameters. To date, no model of this scale has been estimated using the LTE. The most commonly used algorithm, the random walk Metropolis–Hastings algorithm (and its variant), is neither scalable nor numerically stable (Yin, 2009; Yin et al., 2011; Tanaka, 2018). While Brignone et al. (2023) employ a sequential Monte Carlo sampler, it is only feasible for models with a limited number of parameters (e.g., fewer than 10). Further, despite being considered state-of-the-art, the author’s attempt to use Hamiltonian Monte Carlo, as in Hong et al. (2021), proves ineffective for overcoming this problem. This study introduces a generalized elliptical slice sampler (GESS) (Nishihara et al., 2014) and an approximate Gibbs sampler (AGS) tailored for the inference of LPs with the LTE. While the former is exact, it is only applicable to cases with sufficiently non-informative priors. By contrast, the latter is approximate but accommodates informative priors. The posterior distributions simulated using the GESS and AGS do not substantially differ, suggesting that the AGS can be considered a virtually exact algorithm.

The remainder of the paper is organized as follows. In Section 2, we discuss the LTE for LPs, posterior simulation, and estimation of simultaneous credible bands. Through a simulation study, we also demonstrate that the proposed approach works in practice. In Section 3, the approach is extended to the IV method and its statistical properties are examined through a series of Monte Carlo experiments. In Section 4, we apply the proposed approach to analyze monetary policy in the United States. Section 5 concludes.

2 Quasi-Bayesian Inference of LPs

2.1 LPs and the pseudo-posterior

LPs are a sequence of regression equations that captures the relationship between a response variable observed at different horizons, $y_t, y_{t+1}, \dots, y_{t+H}$, and J regressors, \mathbf{x}_t . Specifically, the model is given by

$$y_{t+h} = \boldsymbol{\theta}_{(h)}^\top \mathbf{x}_t + u_{(h),t+h}, \quad h = 0, 1, \dots, H; t = 1, \dots, T, \quad (1)$$

³Recently, Huber et al. (2024) proposed a Bayesian approach to LP-IV. However, their method has two statistical shortcomings. First, as it is a direct extension of the approach proposed by Tanaka (2020a), it inherits the same issue, namely, that the posterior is misspecified, rendering the obtained posterior draws unsuitable for analysis. Second, their approach does not account for the correlations between the error terms in the first-stage (i.e., the regression on an IV) and second-stage equations (i.e., the regressions on the response variables).

where $\boldsymbol{\theta}_{(h)} = (\theta_{1,(h)}, \dots, \theta_{J,(h)})^\top$ denotes a vector of coefficients and $u_{(h),t+h}$ is the error term. The vector of regressors, \mathbf{x}_t , includes a pre-identified exogenous shock (treatment), an intercept, up to L lags of y_t , and other control variables. We assume that the first entry of $\boldsymbol{\theta}_{(h)}$, $\theta_{1,(h)}$, represents the structural shock of interest. Thus, the sequence $\theta_{1,(0)}, \theta_{1,(1)}, \dots, \theta_{1,(H)}$ corresponds to the IRF under study. As shown in Appendix A of Jordà et al. (forthcoming), even when L is smaller than the true lag length of the underlying DGP, the coefficients of LPs are consistently estimated. This contrasts with vector autoregressions in which a truncated lag length can introduce severe bias (Kilian, 1998).

One can also use a long differenced (LD) specification in which the left-hand side of each LP is replaced with a cumulated difference (Stock and Watson, 2018):

$$y_{t+h} - y_t = \boldsymbol{\theta}_{(h)}^\top \mathbf{x}_t^{LD} + u_{(h),t+h}, \quad h = 0, 1, \dots, H; t = 1, \dots, T. \quad (2)$$

The vector of regressors, \mathbf{x}_t^{LD} , is similarly defined as \mathbf{x}_t in the level specification, except that the lags of y_t are replaced by the lags of the first difference of y_t , $y_{t-1} - y_{t-2}, y_{t-2} - y_{t-3}, \dots$. Inference for this specification is conducted in the same way as for the level specification. Piger and Stockwell (2025) argue that this specification can substantially reduce estimation bias and improve confidence interval coverage. While we focus on the level specification for brevity, the LD specification is preferred for use in finite samples, as shown by our simulation study presented in Section 2.5.

In existing studies on Bayesian LPs (Tanaka, 2020a; Ferreira et al., forthcoming), LPs are stacked into a system of equations, similar to a seemingly unrelated regression (Zellner, 1962), and the error terms are *assumed* to follow a multivariate normal distribution with covariance matrix $\boldsymbol{\Sigma}$:

$$\mathbf{y}_t = \boldsymbol{\Theta}^\top \mathbf{x}_t + \mathbf{u}_t, \quad \mathbf{u}_t \sim \mathcal{N}(\mathbf{0}_{H+1}, \boldsymbol{\Sigma}),$$

where $\mathbf{y}_t = (y_t, y_{t+1}, \dots, y_{t+H})^\top$, $\boldsymbol{\Theta} = (\boldsymbol{\theta}_{(0)}, \boldsymbol{\theta}_{(1)}, \dots, \boldsymbol{\theta}_{(H)})$, and $\mathbf{u}_t = (u_t, u_{t+1}, \dots, u_{t+H})^\top$. Define $\boldsymbol{\theta} = \text{vec}(\boldsymbol{\Theta})$, where $\text{vec}(\cdot)$ denotes the column-wise vectorization operator. This approach yields the pseudo-likelihood function in the following standard form:

$$\tilde{\mathcal{L}}(\boldsymbol{\theta}) = (2\pi)^{-\frac{J(H+1)}{2}} |\boldsymbol{\Sigma}|^{-\frac{1}{2}} \exp \left\{ -\frac{1}{2} \sum_{t=1}^T (\mathbf{y}_t - \boldsymbol{\Theta}^\top \mathbf{x}_t)^\top \boldsymbol{\Sigma}^{-1} (\mathbf{y}_t - \boldsymbol{\Theta}^\top \mathbf{x}_t) \right\}.$$

Then, the pseudo-posterior is given by

$$\tilde{\pi}(\boldsymbol{\theta}, \boldsymbol{\Sigma}) \propto |\boldsymbol{\Sigma}|^{-\frac{1}{2}} \exp \left\{ -\frac{1}{2} \sum_{t=1}^T (\mathbf{y}_t - \boldsymbol{\Theta}^\top \mathbf{x}_t)^\top \boldsymbol{\Sigma}^{-1} (\mathbf{y}_t - \boldsymbol{\Theta}^\top \mathbf{x}_t) \right\} p(\boldsymbol{\theta}, \boldsymbol{\Sigma}), \quad (3)$$

where $p(\boldsymbol{\theta}, \boldsymbol{\Sigma})$ denotes a joint prior of $\boldsymbol{\theta}$ and $\boldsymbol{\Sigma}$, while $\mathcal{D} = \{\mathbf{Y}, \mathbf{X}\}$ denotes the set of observations, with $\mathbf{Y} = (\mathbf{y}_1, \dots, \mathbf{y}_T)^\top$ and $\mathbf{X} = (\mathbf{x}_1, \dots, \mathbf{x}_T)^\top$.

Although the point estimator (e.g., posterior mean) of $\boldsymbol{\theta}$ may be consistent, its uncertainty quantification is unsuitable for interval estimation and hypothesis testing because the posterior is not “well calibrated.” Specifically, the spread of the posterior distribution is inaccurately specified, meaning that the resulting credible interval may not possess the nominal coverage property. In other words, 90% credible intervals may not cover the true value with a 90% probability.

Ferreira et al. (forthcoming) propose applying the sandwich covariance matrix estimator of Müller (2013) to LPs, thereby treating each equation separately. This estimator uses only a point estimate (e.g., posterior mean) and the approach is justified by asymptotic theory. However,

methods that rely on the pseudo-likelihood continue to suffer two issues. First, the contribution of the pseudo-likelihood to the posterior is incorrectly evaluated, meaning the inference of θ cannot be considered a proper belief update. Not only does the approach based on the pseudo-likelihood fail to provide interval estimates, but it also does not generate valid point estimates. Second, Ferreira et al.'s (forthcoming) approach cannot estimate simultaneous credible bands, as it performs uncertainty quantification equation by equation (although treats LPs as a single system during posterior simulation). One possible solution to these issues is to modify the pseudo-likelihood by introducing a learning rate (also known as a scaling parameter), $\eta (> 0)$, as seen in generalized/Gibbs posterior inference:⁴

$$\tilde{\pi}_\eta(\theta, \Sigma) \propto \left[|\Sigma|^{-\frac{1}{2}} \exp \left\{ -\frac{1}{2} \sum_{t=1}^T (\mathbf{y}_t - \Theta^\top \mathbf{x}_t)^\top \Sigma^{-1} (\mathbf{y}_t - \Theta^\top \mathbf{x}_t) \right\} \right]^\eta p(\theta, \Sigma).$$

However, while there are various methods for selecting η , none of these are directly applicable to our context.⁵

2.2 The quasi-posterior

In this study, we propose inferring LPs using the LTE (Kim, 2002; Chernozhukov and Hong, 2003), which infers unknown parameters using a set of moment conditions, $\mathbb{E}[\mathbf{m}_t(\theta)] = \mathbf{0}$, where $\mathbf{m}_t(\theta)$ denotes a vector-valued function, known as a moment function. The moment function for LPs is specified as

$$\mathbf{m}_t(\theta) = \begin{pmatrix} (y_t - \theta_{(0)}^\top \mathbf{x}_t) \mathbf{x}_t \\ (y_{t+1} - \theta_{(1)}^\top \mathbf{x}_t) \mathbf{x}_t \\ \vdots \\ (y_{t+H} - \theta_{(H)}^\top \mathbf{x}_t) \mathbf{x}_t \end{pmatrix}.$$

The quasi-likelihood is composed from a GMM criterion (Hansen, 1982) as

$$\mathcal{L}_{\text{LTE}}(\theta) \propto |\mathbf{W}|^{\frac{1}{2}} \exp \left\{ -\frac{T}{2} \bar{\mathbf{m}}(\theta)^\top \mathbf{W} \bar{\mathbf{m}}(\theta) \right\},$$

with

$$\bar{\mathbf{m}}(\theta) = \frac{1}{T} \sum_{t=1}^T \mathbf{m}_t(\theta),$$

where $\bar{\mathbf{m}}(\theta)$ is the empirical mean of the moment functions and \mathbf{W} is a symmetric positive definite weighting matrix. The quasi-posterior is then defined as

$$q(\theta) \propto |\mathbf{W}|^{\frac{1}{2}} \exp \left\{ -\frac{T}{2} \bar{\mathbf{m}}(\theta)^\top \mathbf{W} \bar{\mathbf{m}}(\theta) \right\} p(\theta). \quad (4)$$

Posterior draws are simulated using a standard Bayesian technique such as Markov chain Monte Carlo. The posterior simulation method is discussed later.

It is desirable to update \mathbf{W} along with θ at every cycle of posterior simulation as performed by, for example, Yin (2009). This implies that \mathbf{W} is treated as a function of θ , leading to the following quasi-posterior:

$$q(\theta) \propto |\mathbf{W}(\theta)|^{\frac{1}{2}} \exp \left\{ -\frac{T}{2} \bar{\mathbf{m}}(\theta)^\top \mathbf{W}(\theta) \bar{\mathbf{m}}(\theta) \right\} p(\theta).$$

⁴See Martin and Syring (2022) for an overview.

⁵See Wu and Martin (2023) and the citations therein.

However, such a strategy requires repeated matrix inversions to compute $\mathbf{W}(\boldsymbol{\theta})$, making the posterior simulation computationally demanding and unstable (Yin et al., 2011; Tanaka, 2018). To address this issue, we fix \mathbf{W} to be the sample precision matrix of the moment function evaluated at some estimate of $\boldsymbol{\theta}$, denoted as $\boldsymbol{\theta}^*$, based on the sample at hand. A natural choice for $\boldsymbol{\theta}^*$ is the ordinary least squares (OLS) estimator:

$$\hat{\boldsymbol{\theta}}^{\text{OLS}} = \text{vec} \left((\mathbf{X}^\top \mathbf{X})^{-1} \mathbf{X}^\top \mathbf{Y} \right).$$

While Herbst and Johannsen (2024) propose a bias-corrected estimator for LPs, Li et al. (2024) argue that such an estimator should only be used when correcting bias because of the substantial bias/variance trade-off involved. In this study, we use the OLS estimator rather than the bias-corrected estimator for the following reasons. First, while the bias-corrected estimator reduces bias, it also inflates the estimation error (e.g., mean squared error). Second, based on a battery of simulation studies, Li et al. (2024, p. 2) conclude that “of all the estimators we consider, bias-corrected LP is the preferred option if and only if the loss function almost exclusively puts weight on bias (at the expense of variance).” Although not reported here, we find that using the bias-corrected estimator to set \mathbf{W} has a negligible effect on posterior inference.⁶

When \mathbf{W} is not optimally chosen, the posterior covariance matrix is evaluated based on an asymptotic argument (Chernozhukov and Hong, 2003; Kormilitsina and Nekipelov, 2016; Hong et al., 2021). The asymptotic distribution of $\hat{\boldsymbol{\theta}}$ is a multivariate normal distribution given by

$$\sqrt{T} \left(\hat{\boldsymbol{\theta}} - \boldsymbol{\theta}^{\text{true}} \right) \xrightarrow{d} \mathcal{N}(\mathbf{0}_D, \boldsymbol{\Omega}_0), \quad \text{as } T \rightarrow \infty,$$

where

$$\boldsymbol{\Omega}_0 = (\mathbf{G}^\top \mathbf{W} \mathbf{G})^{-1} \mathbf{G}^\top \mathbf{W} \mathbf{V}(\boldsymbol{\theta}^{\text{true}}) \mathbf{W} \mathbf{G} (\mathbf{G}^\top \mathbf{W} \mathbf{G})^{-1}, \quad (5)$$

and

$$\mathbf{G} = \nabla_{\boldsymbol{\theta}} \bar{\mathbf{m}}(\boldsymbol{\theta}^{\text{true}}) = \mathbf{I}_{H+1} \otimes \left(-\frac{1}{T} \mathbf{X}^\top \mathbf{X} \right).$$

Here, $\boldsymbol{\theta}^{\text{true}}$ is the true value of $\boldsymbol{\theta}$, $\mathbf{V}(\boldsymbol{\theta}^{\text{true}})$ is the covariance matrix of the moment function evaluated at $\boldsymbol{\theta}^{\text{true}}$, and ∇ denotes the gradient operator. In practice, $\mathbf{V}(\boldsymbol{\theta}^{\text{true}})$ is replaced by an estimate based on the sample estimate $\hat{\boldsymbol{\theta}}$, denoted as $\mathbf{V}(\hat{\boldsymbol{\theta}})$. When the sample size is sufficiently large and/or the contribution of the prior to the posterior is negligible, this posterior covariance estimator is comparable to the sandwich variance estimator for GMM (and OLS).

One may consider using the heteroskedasticity- and autocorrelation-robust (HAR) covariance estimator (Newey and West, 1987; Lazarus et al., 2018) to estimate $\mathbf{V}(\hat{\boldsymbol{\theta}})$. However, Montiel Olea and Plagborg-Møller (2021) show that when LPs augment lagged responses, it is unnecessary to use an autocorrelation-robust estimator for inference in LPs. Given the asymptotic property of the LTE is closely related to its frequentist counterpart, their argument applies to the LTE. We confirm this point through a simulation study, as shown in Section 2.5.

While the covariance estimator mentioned above is the standard tool for the LTE, inference of LPs is an exception: we do not need to rely on the asymptotic argument and can instead use simulated posterior draws directly. When $\boldsymbol{\theta}^* = \boldsymbol{\theta}^{\text{true}}$, and thus $\mathbf{W}(\boldsymbol{\theta}^{\text{true}}) = \mathbf{V}(\boldsymbol{\theta}^{\text{true}})^{-1}$, the asymptotic covariance matrix reduces to the inverse of the Hessian of the log quasi-likelihood evaluated at $\boldsymbol{\theta}^{\text{true}}$,

$$\boldsymbol{\Omega}_0 = (\mathbf{G}^\top \mathbf{W}(\boldsymbol{\theta}^{\text{true}}) \mathbf{G})^{-1}.$$

⁶This result is available upon request.

This implies that as long as a good estimator for θ^* is available, we can treat the quasi-likelihood as a “proper” likelihood. Therefore, when $\theta^* = \hat{\theta}^{\text{OLS}}$, simulated draws can be used for posterior analysis. The simulation study shows that when a non-informative prior is used, there is no difference between credible intervals based on the sandwich estimator (5) and those based on simulated draws. Moreover, credible intervals derived from simulated draws achieve the nominal frequentist coverage probability, meaning that the quasi-likelihood is “well calibrated.”

2.3 Posterior simulator

Even when \mathbf{W} is fixed, posterior simulation for LPs using the LTE remains challenging because of the large number of unknown parameters to be inferred. In this study, we propose two computational strategies: the GESS and AGS. Both have advantages and disadvantages. The GESS is exact and accommodates arbitrary priors but is only applicable to cases with sufficiently non-informative (arbitrary) priors. On the contrary, the AGS is approximate and accommodates only a limited class of priors but is feasible for cases with informative priors.

First, we propose using the GESS (Nishihara et al., 2014) for posterior simulation (Algorithm 1). The GESS builds on the elliptical slice sampler (Murray et al., 2010) that is designed to sample from a posterior with an arbitrary likelihood and normal prior. A single step of the elliptical slice sampler involves three key steps: given the current state, (1) a random ellipse is chosen from the normal prior, (2) a level set is randomly selected, and a bracket for sampling is defined, and (3) the next state of the Markov chain is simulated on the intersection of the ellipse and level set by repeatedly shrinking the bracket until the next state is accepted. The elliptical slice sampler is computationally efficient because it avoids repeated matrix inversions, unlike a Gibbs sampler, and offers dimension-independent performance (Nesterov, 2009).

The GESS is an extension of the elliptical slice sampler designed to handle arbitrary priors. We follow Nishihara et al. (2014) and reframe the target kernel as

$$q(\boldsymbol{\theta}) = \frac{q(\boldsymbol{\theta})}{f_N(\boldsymbol{\theta}|\boldsymbol{\mu}, \boldsymbol{\Upsilon})} \times f_N(\boldsymbol{\theta}|\boldsymbol{\mu}, \boldsymbol{\Upsilon}),$$

where $f_N(\boldsymbol{\theta}|\boldsymbol{\mu}, \boldsymbol{\Upsilon})$ denotes a probability density function of a multivariate normal distribution with mean $\boldsymbol{\mu}$ and covariance matrix $\boldsymbol{\Upsilon}$ evaluated at $\boldsymbol{\theta}$. The first term on the right-hand side, $q(\boldsymbol{\theta})/f_N(\boldsymbol{\theta}|\boldsymbol{\mu}, \boldsymbol{\Upsilon})$, is treated as the “likelihood,” while the second term, $f_N(\boldsymbol{\theta}|\boldsymbol{\mu}, \boldsymbol{\Upsilon})$, is treated as the “prior.” We then apply the original elliptical slice sampler. In this study, we set $\boldsymbol{\mu}$ to θ^* and $\boldsymbol{\Upsilon}$ to $\mathbf{V}(\theta^*)$ because the algorithm is computationally more efficient, as the “prior” is close to the target distribution.⁷

Although rare, the shrinkage process may require a large number of iterations. If this happens, the algorithm can become stuck. To avoid this problem, we terminate the shrinkage process when the iteration reaches a prespecified limit such as 100 and temporarily switch to a random walk Metropolis–Hastings step. In this study, a proposal is drawn from a multivariate distribution with a covariance matrix $\left(2.38/\sqrt{J(H+1)}\right)^2 \boldsymbol{\Upsilon}$. This choice of proposal distribution is based on the theoretical work of Roberts et al. (1997).

⁷Computational efficiency could be improved by setting the “prior” to a multivariate t distribution and tuning it adaptively, as suggested by Nishihara et al. (2014), or by adopting the transport elliptical slice sampler of Cabezas and Nemeth (2023), which uses normalizing flows to map the structure of the target distribution to the standard normal distribution. Since both approaches require a powerful parallel computing environment, we do not consider them in this study.

Algorithm 1 A single step of the GESS for the LTE

Input: Current state θ , Gaussian parameters μ and Υ , log quasi-posterior $\log q(\cdot)$
 $\nu \sim \mathcal{N}(\mu, \Upsilon)$ // Choose an ellipse
 $\varrho \sim \mathcal{U}(0, 1)$
 $\log q^* \leftarrow \log q(\theta|\mathcal{D}) + \log(\varrho)$ // Set a threshold
 $\zeta \sim \mathcal{U}(0, 2\pi)$ // Draw an initial point
 $\zeta_{\min} \leftarrow \zeta - 2\pi, \zeta_{\max} \leftarrow \zeta$ // Define a bracket
while converge
 $\text{vec}(\theta') \leftarrow (\theta - \mu) \cos(\zeta) + (\nu - \mu) \sin(\zeta) + \mu$ // Get a proposal
 if $\log q(\theta'|\mathcal{D}) - 0.5(\theta' - \mu)^\top \Upsilon^{-1}(\theta' - \mu) > \log q^*$ then:
 break
 else:
 // Shrink the bracket
 if $\zeta < 0$ then:
 $\zeta_{\min} \leftarrow \zeta$
 else:
 $\zeta_{\max} \leftarrow \zeta$
 end if
 $\zeta \sim \mathcal{U}(\zeta_{\min}, \zeta_{\max})$ // Draw a next point
 end if
end while
return θ'

Second, we introduce the AGS to handle informative priors. Suppose a prior of θ has the following structure:

$$p(\theta|\tau) \propto \exp\left(-\frac{1}{2}\theta^\top \mathbf{Q}_\tau \theta\right),$$

where τ denotes a vector of hyperparameters and \mathbf{Q}_τ is a symmetric positive definite matrix that depends on τ . This class of priors encompasses all the prior specifications considered in the literature, including the roughness-penalty prior (Tanaka, 2020a), normal-gamma prior (Ferreira et al., forthcoming; Brugnolini et al., 2024), and Gaussian process prior (Huber et al., 2024). Since the asymptotic mean and covariance matrix of the LTE does not depend on θ , we can interpret the asymptotic distribution of the LTE as the probabilistic model for θ :

$$\theta \sim \mathcal{N}(\theta^*, \Omega(\theta^*)), \quad \text{with } \Omega(\theta^*) = \frac{1}{T} (\mathbf{G}^\top \mathbf{W}(\theta^*) \mathbf{G})^{-1}.$$

This constitutes a normal likelihood:

$$\check{\mathcal{L}}(\mathcal{D}|\theta) = f_N(\theta|\theta^*, \Omega(\theta^*)),$$

which leads to the following quasi-posterior:

$$q(\theta, \tau) \propto \check{\mathcal{L}}(\mathcal{D}|\theta) p(\theta|\tau) p(\tau),$$

where $p(\tau)$ denotes the prior density of τ .⁸ The conditional posterior of θ is given by

$$\theta|\tau \sim \mathcal{N}\left(\left(\Omega(\theta^*)^{-1} + \mathbf{Q}\right)^{-1} \Omega(\theta^*)^{-1} \theta^*, \left(\Omega(\theta^*)^{-1} + \mathbf{Q}\right)^{-1}\right).$$

In Section 2.5, we empirically confirm that the GESS and AGS generate virtually identical posterior distributions.

The relative computational performance of the GESS and AGS depends on the informativeness of the prior or, equivalently, the discrepancy between the (conditional) posterior of θ and $f_N(\theta|\mu, \Upsilon)$. When the prior is sufficiently non-informative, the GESS is more efficient because it does not require repeated matrix inversions. However, as the prior becomes more informative, the performance of the GESS deteriorates exponentially. While the AGS experiences a similar issue, it remains fairly robust.

2.4 Simultaneous credible band

In our framework, a simultaneous credible band can be computed using the method proposed by Montiel Olea and Plagborg-Møller (2019). A simultaneous $1 - \alpha$ credible band for the coefficients of a structural shock, $\theta_1 = (\theta_{1,(0)}, \theta_{1,(1)}, \dots, \theta_{1,(H)})$, is given by the Cartesian product of intervals as

$$\hat{\mathcal{C}} = \prod_{h=0}^H \hat{\mathcal{C}}_{(h)},$$

where $\hat{\mathcal{C}}_h$ denotes an interval such that the true value of θ_1 , denoted by θ_1^{true} , is asymptotically covered with a probability of at least $1 - \alpha$:

$$\liminf_{T \rightarrow \infty} P\left(\theta_1^{\text{true}} \in \hat{\mathcal{C}}\right) = \liminf_{T \rightarrow \infty} P\left(\theta_{1,(h)}^{\text{true}} \in \hat{\mathcal{C}}_{(h)} \text{ for } h = 0, 1, \dots, H\right) \geq 1 - \alpha.$$

Let $\hat{\Omega}_1$ denote the estimated posterior covariance matrix for θ_1 , obtained by deleting the rows and columns irrelevant to θ_1 from the full posterior covariance matrix. Let $\hat{\zeta}_{(h)}$ denote the point-wise standard error for $\theta_{1,(h)}$, which is computed as

$$\hat{\zeta}_{(h)} = T^{-\frac{1}{2}} \sqrt{\hat{\Omega}_{1,(h,h)}},$$

where $\hat{\Omega}_{1,(h,h)}$ denotes the $(h + 1)$ th diagonal element of $\hat{\Omega}_1$. Given a critical value c , a credible band is defined as

$$\hat{\mathcal{B}}(c) = \hat{B}\left(\hat{Q}_{1-\alpha}\right) = \times_{h=0}^H \left[\hat{\theta}_{1,(h)} - \hat{\zeta}_{(h)}c, \hat{\theta}_{1,(h)} + \hat{\zeta}_{(h)}c\right].$$

Montiel Olea and Plagborg-Møller (2019) propose two implementation algorithms to find c . The first algorithm, referred to as the plug-in sup-t algorithm, takes a plug-in approach: random vectors are generated from a multivariate normal distribution with mean zero and covariance matrix $\hat{\Omega}_1$, and then c is chosen using the draws (Algorithm 2):

$$c = Q_\xi \left(\max_{h=0,1,\dots,H} \left| \hat{\Omega}_{1,(h,h)}^{-\frac{1}{2}} e^{(h)} \right| \right),$$

⁸Our inferential approach is closely related to that of Hahn et al. (2019), who reframe the likelihood of a normal linear regression to a normal model of regression coefficients and apply the GESS, treating it as the “prior” and the prior density as the “likelihood.” Analogously, we can apply the GESS to this quasi-posterior by treating $\check{\mathcal{L}}(\mathcal{D}|\theta)$ as the “prior” and $p(\theta|\tau)$ as the “likelihood.” However, based on the author’s experience, this computational strategy does not perform well with a highly informative prior.

Algorithm 2 Plug-in sup-t algorithm

input : Estimate of the posterior covariance of θ_1 , $\hat{\Omega}_1$

Draw $e^{(t)} \sim \mathcal{N}(\mathbf{0}_{H+1}, \hat{\Omega}_1)$, $t = 1, \dots, T$.

Define $c = \hat{Q}_{1-\alpha}$ as the empirical $1-\alpha$ quantile of $\max_{h=0,1,\dots,H} \left| \hat{\Omega}_{1,(h,h)}^{-\frac{1}{2}} e^{(t)} \right|$ across $t = 1, \dots, T$.

Set $\hat{\mathcal{C}} = \times_{h=0}^H \left[\hat{\theta}_{1,(h)} - \hat{\zeta}_{(h)}c, \hat{\theta}_{1,(h)} + \hat{\zeta}_{(h)}c \right]$.

return $\hat{\mathcal{C}}$

Algorithm 3 Quantile-based sup-t algorithm

input : N posterior draws of θ_1 , $\left\{ \theta_1^{(n)} = \left(\theta_{1,(0)}^{(n)}, \theta_{1,(1)}^{(n)}, \dots, \theta_{1,(H)}^{(n)} \right)^\top : n = 1, \dots, N \right\}$

Define $\hat{Q}_{(h),\xi}$ as the empirical ξ quantile of $\theta_{1,(h)}^{(1)}, \dots, \theta_{1,(h)}^{(N)}$.

Obtain $\hat{\xi}$ by numerically solving $N^{-1} \sum_{n=1}^N \mathbb{I} \left(\hat{\theta}_1 \in \times_{h=0}^H \left[\hat{Q}_{(h),\xi}, \hat{Q}_{(h),1-\xi} \right] \right) = 1 - \alpha$.

Set $\hat{\mathcal{C}} = \times_{h=0}^H \left[\hat{Q}_{(h),\hat{\xi}}, \hat{Q}_{(h),1-\hat{\xi}} \right]$.

return $\hat{\mathcal{C}}$

$$e = (e_{(0)}, e_{(1)}, \dots, e_{(H)})^\top \sim \mathcal{N}(\mathbf{0}_{H+1}, \hat{\Omega}_1),$$

where e denotes an auxiliary random vector and $Q_\xi(\cdot)$ denotes the ξ -quantile function. The second algorithm, referred to as the quantile-based sup-t algorithm, directly uses the posterior draws for θ_1 obtained from a posterior simulation (Algorithm 3). A desirable value of $\hat{\xi}$ can be found using a root-finding algorithm.⁹ Montiel Olea and Plagborg-Møller (2019) show that the two algorithms are asymptotically equivalent.

2.5 Simulation study

To compare the frequentist properties of the proposed approach with those of existing ones, we conducted a simulation study. We generated synthetic data from the following vector moving average process:

$$\mathbf{w}_t = \sum_{l=0}^L \Gamma_l \boldsymbol{\varepsilon}_{t-l}, \quad \boldsymbol{\varepsilon}_t \sim \mathcal{N}(\mathbf{0}_M, \mathbf{I}_M),$$

where $\mathbf{w}_t = (w_{1,t}, \dots, w_{M,t})^\top$ denotes a vector of observations and $\boldsymbol{\varepsilon}_t = (\varepsilon_{1,t}, \dots, \varepsilon_{M,t})^\top$ denotes a vector of independently and identically distributed structural shocks. The primary objective of the inference was to estimate the responses of the second variable, $w_{2,t}, w_{2,t+1}, \dots, w_{2,t+H}$, to the first structural shock, $\varepsilon_{1,t}$. Let $\gamma_{m,m',l}$ denote the (m, m') entry of Γ_l . The first entry of \mathbf{w}_t was set to a pre-identified structural shock, $w_{1,t} = \varepsilon_{1,t}$. Thus, we set $\gamma_{1,1,0} = 1$ and the first rows of Γ_l were all zero for $l = 1, \dots, L$. The sequence of $(2, 1)$ entries of Γ_l represented the IRF, which was specified as

$$\gamma_{2,1,l} = \frac{(l+1) \exp(0.5(1-l))}{\sum_{l=1}^L (l+1) \exp(0.5(1-l))}, \quad l = 0, 1, \dots, L.$$

⁹In this study, we use the Matlab function `fzero`.

Figure 1: Impulse response function

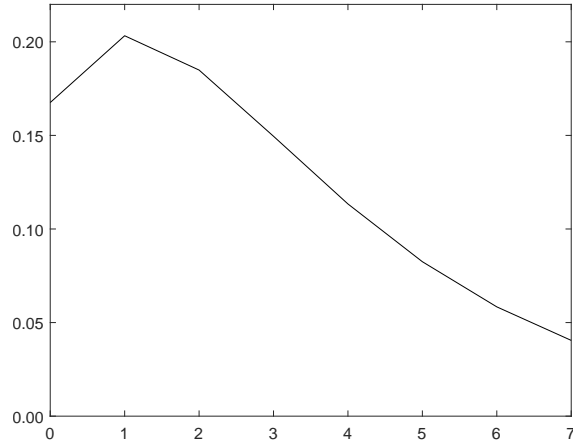


Figure 1 displays the shape of the IRF to be inferred. The other entries of Γ_l were specified as

$$\gamma_{m,m',l} = \frac{1}{2} \frac{L+2-l}{L+1} \gamma_{m,m'}^*,$$

where each $\gamma_{m,m'}^*$ was independently generated from a uniform distribution of $(0, 0.5)$. Both level and LD specifications were considered. For the level specification, a regressor, \mathbf{x}_t , included an intercept, the current structural shock, $\varepsilon_{1,t}$ ($= w_{1,t}$), and the L lags of the observations, $\mathbf{w}_{t-1}, \dots, \mathbf{w}_{t-L}$. For the LD specification, \mathbf{x}_t was specified similarly, but the lags of $w_{2,t}$ were replaced by their first differences. We considered three cases for time series length $T \in \{200, 500, 1000\}$, while fixing $H = L = 7$. In total, 1,000 synthetic datasets were generated.

We considered four alternative approaches in which a non-informative prior was employed in all cases to minimize the influence of priors on the posterior. Specifically, we assigned a flat prior to $\boldsymbol{\theta}$, $p(\boldsymbol{\theta}) \propto 1$, and where necessary, a scale-invariant Jeffreys prior to $\boldsymbol{\Sigma}$, $p(\boldsymbol{\Sigma}) \propto |\boldsymbol{\Sigma}|^{-(H+2)/2}$.

Pseudo-raw The first approach (Pseudo-raw) used the pseudo-likelihood from Tanaka (2020a), where the posterior draws were simulated using a Gibbs sampler. The conditional posterior of $\boldsymbol{\theta}$ is specified as

$$\begin{aligned} \boldsymbol{\theta} | \boldsymbol{\Sigma} &\sim \mathcal{N}(\mathbf{m}, \mathbf{P}^{-1}), \\ \mathbf{m} &= \mathbf{P}^{-1} (\boldsymbol{\Sigma}^{-1} \otimes \mathbf{X}^\top) \text{vec}(\mathbf{Y}), \\ \mathbf{P} &= \boldsymbol{\Sigma}^{-1} \otimes \mathbf{X}^\top \mathbf{X}, \\ \boldsymbol{\Sigma} | \boldsymbol{\theta} &\sim \mathcal{IW}\left(T, (\mathbf{Y} - \mathbf{X}\boldsymbol{\theta})^\top (\mathbf{Y} - \mathbf{X}\boldsymbol{\theta})\right), \end{aligned}$$

where $\mathcal{IW}(a, \mathbf{B})$ denotes an inverse Wishart distribution with a degrees of freedom and scale matrix \mathbf{B} . As in Tanaka (2020a), $\boldsymbol{\theta}$ was simulated using an algorithm described in Section 2 of Rue (2001), which is faster and more stable than a naive implementation. Credible intervals were obtained by computing the 5th and 95th percentiles of the simulated draws.

Pseudo-sand The second and third approaches used the same draws as Pseudo-raw, but the posterior variances were computed using the sandwich estimator of Müller (2013) for each LP, as outlined in Ferreira et al. (forthcoming). The covariance estimator, written in our notation, is given by

$$\hat{\mathbf{V}}[\boldsymbol{\theta}_{(h)}] = T (\mathbf{X}^\top \mathbf{X})^{-1} \hat{\mathbf{V}}_{(h)} (\mathbf{X}^\top \mathbf{X})^{-1},$$

where $\hat{\boldsymbol{\theta}}_{(h)}$ denotes a posterior mean estimate of $\boldsymbol{\theta}_{(h)}$ and $\hat{\mathbf{V}}$ is an estimate of the covariance matrix of the point estimate. We considered two estimators for $\hat{\mathbf{V}}$. The first is the HAR covariance estimator of Newey and West (1987) given by

$$\hat{\mathbf{V}}_{(h)} = \hat{\mathbf{B}}_{(h),0} + \sum_{s=1}^S \left(1 - \frac{s}{S+1}\right) \left(\hat{\mathbf{B}}_{(h),s} + \hat{\mathbf{B}}_{(h),s}^\top\right),$$

$$\hat{\mathbf{B}}_{(h),s} = \frac{1}{T} \sum_{t=s+1}^T \hat{u}_{(h),t+h} \hat{u}_{(h),t+h-s} \mathbf{x}_t \mathbf{x}_{t-s}^\top,$$

$$\hat{u}_{(h),t+h} = y_{t+h} - \hat{\boldsymbol{\theta}}_{(h)}^\top \mathbf{x}_{t-1},$$

where S denotes the bandwidth. The use of this estimator was suggested by Ferreira et al. (forthcoming). We selected $S = \lceil 1.3T^{1/2} \rceil$, following the recommendation of Lazarus et al. (2018), where $\lceil \cdot \rceil$ denotes the nearest integer operator. The second is the standard covariance estimator:

$$\hat{\mathbf{V}}_{(h)} = \frac{1}{T} \sum_{t=s+1}^T \hat{u}_{(h),t+h} \hat{u}_{(h),t+h-s} \mathbf{x}_t \mathbf{x}_{t-s}^\top.$$

LTE-raw The fourth and fifth approaches were based on the LTE. Posterior draws were simulated from the quasi-posterior using the GESS and credible intervals were estimated as the intervals between the 5th and 95th percentiles of the draws. When computing \mathbf{W} and $\mathbf{V}(\hat{\boldsymbol{\theta}})$, we used the standard covariance matrix estimator and the HAR covariance estimator of Newey and West (1987).

LTE-sand The sixth and seventh approaches relied on the same draws as LTE-raw but evaluated the credible intervals using the asymptotic covariance estimator.

A total of 50,000 draws were simulated and the last 40,000 draws were used for posterior analysis.¹⁰ We computed the following performance measures:

- Median bias of the posterior mean (Bias),
- Median absolute error of the posterior mean (MAE),
- Median length of the point-wise 90% credible interval (Length),
- Coverage probability of the point-wise 90% credible interval (P-Coverage),
- Coverage probability of the simultaneous 90% credible band (S-Coverage),
- Median of the minimum effective sample sizes per iteration (minESS/iter),
- Median of the minimum effective sample sizes per second (minESS/s).

Tables 1 and 2 summarize the results for Bias and MAE. Three key points are worth noting:

¹⁰All the programs were executed in Matlab (R2024b) on an Ubuntu desktop (22.04.5 LTS) running on an AMD Ryzen Threadripper 3990X 2.9 GHz 64-core processor.

Table 1: Simulation results for LPs (1): Median bias

T	Spec.	Method	h							
			0	1	2	3	4	5	6	7
200	Level	Pseudo	.0000	-.0009	-.0038	-.0067	-.0065	-.0070	-.0071	-.0080
		LTE	.0000	-.0009	-.0038	-.0068	-.0064	-.0072	-.0068	-.0082
	LD	Pseudo	.0010	-.0014	.0002	-.0010	-.0019	-.0023	-.0020	-.0025
		LTE	.0009	-.0013	.0002	-.0012	-.0018	-.0023	-.0022	-.0026
500	Level	Pseudo	.0003	-.0002	-.0007	-.0015	-.0017	-.0027	-.0022	-.0027
		LTE	.0003	-.0001	-.0007	-.0014	-.0015	-.0027	-.0023	-.0027
	LD	Pseudo	-.0002	-.0000	-.0012	-.0010	-.0006	-.0007	-.0005	-.0010
		LTE	-.0001	.0000	-.0011	-.0009	-.0006	-.0006	-.0005	-.0010
1,000	Level	Pseudo	-.0000	-.0004	-.0011	-.0011	-.0011	-.0003	-.0001	-.0006
		LTE	-.0000	-.0004	-.0011	-.0011	-.0012	-.0003	-.0002	-.0006
	LD	Pseudo	.0001	.0001	.0000	-.0001	-.0003	-.0006	-.0008	-.0009
		LTE	.0001	.0001	.0003	-.0002	-.0003	-.0006	-.0008	-.0010

Table 2: Simulation results for LPs (2): Median absolute error

T	Spec.	Method	h							
			0	1	2	3	4	5	6	7
200	Level	Pseudo	.011	.017	.022	.026	.027	.029	.029	.028
		LTE	.011	.018	.022	.026	.027	.029	.029	.028
	LD	Pseudo	.012	.018	.023	.028	.031	.033	.034	.034
		LTE	.012	.018	.023	.028	.031	.033	.034	.034
500	Level	Pseudo	.004	.007	.010	.012	.013	.014	.014	.014
		LTE	.004	.007	.010	.012	.013	.014	.014	.014
	LD	Pseudo	.004	.007	.010	.011	.013	.014	.014	.015
		LTE	.004	.007	.010	.011	.013	.014	.014	.015
1,000	Level	Pseudo	.002	.004	.006	.008	.009	.009	.009	.008
		LTE	.002	.004	.006	.008	.009	.009	.009	.009
	LD	Pseudo	.002	.004	.006	.007	.008	.009	.009	.009
		LTE	.002	.004	.006	.007	.008	.009	.009	.009

1. The performance of the point estimation did not differ significantly between Pseudo-raw/sand and LTE-raw/sand. This was expected given the asymptotic consistency of both approaches.
2. The LD specification exhibited smaller bias than the level specification, especially for longer projection horizons. Additionally, the bias in the level specification decreased as the sample size increased.
3. Despite the reduced bias, the MAE for the LD specification was comparable to that for the level specification.

The last two observations are consistent with the arguments made by Herbst and Johansen (2024); Piger and Stockwell (2025).

Tables 3 and 4 summarize the results for Length and P-Coverage. Four key points are worth mentioning:

1. Length differed significantly between Pseudo-raw and Pseudo-sand. This suggests that when using the pseudo-likelihood, the sandwich estimator “adjusts” the spread of the posterior. Moreover, the nominal frequentist coverage probability for Pseudo-raw was far from the 90% target; for short (long) projection horizons, the credible intervals tended to be too long (short).
2. The results for LTE-raw and LTE-sand were virtually identical. This implies that when using the LTE, a distribution of simulated draws and its asymptotic counterpart do not differ substantially. In contrast to the pseudo-posterior, the quasi-posterior appeared to be comparatively “well calibrated,” with the relative importance of the likelihood and prior components to the posterior appropriately evaluated.
3. The results for Pseudo-sand and LTE-raw/sand did not differ significantly and they estimated the same posterior distribution when the prior was negligible.
4. The LD specification exhibited better coverage than the level specification. The level specification consistently underestimated the 90% credible intervals. By contrast, the LD specification effectively achieved the nominal coverage, although tended to be overly optimistic for smaller samples.

In summary, the LD specification is statistically less efficient than the level specification, but has less bias and better nominal coverage. This aligns with the argument of Piger and Stockwell (2025).

Tables A.1 and A.2 in the Online Appendix report the results for P-Coverage and S-Coverage with the LTE using the HAR covariance estimator, respectively. When the HAR covariance estimator was used, P-Coverage and S-Coverage were typically below the nominal level, even with a large sample size. As expected from the results in Tables 3 and 4, P-Coverage for Pseudo using the HAR covariance estimator was virtually identical to that for the LTE with that estimator. These results align with the argument made by Montiel Olea and Plagborg-Møller (2021): an autocorrelation-robust covariance estimator should not be used, while the lags of a response variable should be included as regressors.

Table 5 summarizes the results for S-Coverage. The results for both the plug-in and the quantile-based algorithms were close, consistent with the theoretical argument made by Montiel Olea and Plagborg-Møller (2019). Regardless of whether the level or LD specification was used, S-Coverage was generally below the nominal level, especially when the sample size was small. In this regard, the LD specification outperformed the level specification. Table A.2 in the Online Appendix provides the results for S-Coverage with the LTE using the HAR covariance estimator. Similar to the results for P-Coverage, S-Coverage was significantly below the target level. Pseudo with the HAR covariance estimator, corresponding to Ferreira et al.’s (forthcoming) approach, yielded nearly identical results to the LTE with the HAR covariance estimator; in particular, it consistently underestimated the 90% credible intervals.

Table 6 reports the results for the computational efficiency measures. As shown in the left column, minESS/iter for the Gibbs sampler (Pseudo) and the GESS (LTE) were close to 1, indicating that both algorithms generated high-quality chains. However, minESS/s for the GESS was significantly larger than that for the Gibbs sampler, suggesting that the proposed algorithm was much faster than the Gibbs sampler.

In turn, we compared the GESS and AGS using an informative prior. Specifically, θ was inferred using the roughness-penalty prior (Tanaka, 2020a):

$$p(\theta_j | \tau_j) \propto \exp \left\{ -\frac{1}{2\tau_j} \theta_j^\top \mathbf{D}^\top \mathbf{D} \theta_j \right\},$$

Table 3: Simulation results for LPs (3): Length of the point-wise 90% credible interval

T	Spec.	Method	Cov.	h							
				0	1	2	3	4	5	6	7
200	Level	Pseudo	raw	.108	.134	.132	.127	.120	.110	.093	.066
			sand	.051	.077	.097	.109	.117	.121	.123	.123
		LTE	raw	.051	.077	.098	.109	.117	.121	.123	.123
			sand	.051	.077	.097	.109	.117	.121	.123	.123
	LD	Pseudo	raw	.151	.158	.152	.144	.134	.119	.099	.068
			sand	.055	.084	.107	.123	.135	.141	.145	.146
		LTE	raw	.055	.084	.108	.123	.135	.141	.145	.146
			sand	.055	.084	.108	.123	.135	.141	.145	.146
500	Level	Pseudo	raw	.034	.065	.064	.062	.059	.054	.045	.030
			sand	.017	.033	.046	.054	.059	.061	.062	.063
		LTE	raw	.017	.033	.046	.054	.059	.061	.062	.063
			sand	.017	.033	.046	.054	.059	.061	.062	.063
	LD	Pseudo	raw	.051	.069	.068	.066	.062	.056	.046	.030
			sand	.018	.035	.048	.057	.063	.066	.068	.069
		LTE	raw	.018	.035	.048	.058	.063	.066	.068	.069
			sand	.018	.035	.048	.058	.063	.066	.068	.069
1,000	Level	Pseudo	raw	.014	.042	.042	.041	.039	.035	.029	.019
			sand	.007	.020	.029	.035	.038	.040	.041	.042
		LTE	raw	.007	.020	.029	.035	.038	.040	.041	.042
			sand	.007	.020	.029	.035	.038	.040	.041	.042
	LD	Pseudo	raw	.023	.043	.043	.042	.040	.036	.029	.019
			sand	.008	.020	.030	.036	.040	.042	.043	.044
		LTE	raw	.008	.020	.030	.036	.040	.042	.043	.044
			sand	.008	.020	.030	.036	.040	.042	.043	.044

Table 4: Simulation results for LPs (4): Coverage probability of the point-wise 90% credible interval

T	Spec.	Method	Cov.	h							
				0	1	2	3	4	5	6	7
200	Level	Pseudo	raw	.998	.992	.947	.898	.841	.802	.716	.570
			sand	.870	.878	.858	.845	.826	.835	.845	.848
		LTE	raw	.870	.849	.854	.842	.825	.836	.843	.846
			sand	.869	.849	.858	.844	.825	.834	.846	.847
	LD	Pseudo	raw	.999	.996	.963	.935	.875	.812	.689	.512
			sand	.870	.873	.873	.878	.877	.871	.862	.866
		LTE	raw	.868	.871	.875	.878	.879	.870	.862	.865
			sand	.869	.870	.874	.878	.878	.870	.862	.866
500	Level	Pseudo	raw	.999	.996	.978	.927	.895	.829	.742	.541
			sand	.896	.881	.890	.884	.889	.887	.877	.888
		LTE	raw	.895	.881	.890	.885	.887	.887	.877	.889
			sand	.896	.879	.891	.885	.890	.885	.875	.888
	LD	Pseudo	raw	1.000	.997	.978	.936	.903	.847	.739	.528
			sand	.893	.840	.903	.898	.906	.904	.892	.896
		LTE	raw	.895	.893	.902	.896	.903	.904	.893	.892
			sand	.894	.891	.903	.896	.904	.903	.893	.896
1,000	Level	Pseudo	raw	.998	1.000	.973	.930	.880	.820	.742	.548
			sand	.898	.885	.874	.884	.877	.876	.879	.885
		LTE	raw	.896	.885	.874	.883	.873	.875	.878	.887
			sand	.896	.885	.875	.885	.876	.877	.879	.885
	LD	Pseudo	raw	1.000	1.000	.983	.938	.895	.836	.746	.543
			sand	.902	.902	.891	.898	.894	.891	.909	.900
		LTE	raw	.903	.902	.891	.898	.894	.892	.907	.901
			sand	.904	.904	.891	.898	.895	.890	.908	.901

Table 5: Simulation results for LPs (5): Coverage probability of the simultaneous 90% credible band

T	Spec.	Cov.	plug-in	quantile
200	Level	raw	–	.835
		sand	.831	–
	LD	raw	–	.840
		sand	.842	–
500	Level	raw	–	.890
		sand	.891	–
	LD	raw	–	.890
		sand	.892	–
1,000	Level	raw	–	.863
		sand	.864	–
	LD	raw	–	.892
		sand	.892	–

Table 6: Simulation results for LPs (6): Computational efficiency

T	Spec.	Method	minESS/iter	minESS/s
200	Level	Pseudo	.941	1,134
		LTE	.935	14,264
	LD	Pseudo	.940	1,165
		LTE	.936	14,063
500	Level	Pseudo	.941	390
		LTE	.936	6,100
	LD	Pseudo	.942	288
		LTE	.937	5,827
1,000	Level	Pseudo	.941	42
		LTE	.937	2,925
	LD	Pseudo	.943	42
		LTE	.938	2,865

Note: minESS/iter and minESS/s denote the medians of the minimum effective sample sizes per iteration and per second, respectively.

where τ_j is a shrinkage parameter and \mathbf{D} denotes the second-order difference matrix with a dimension of $(H - 1) \times (H + 1)$. The joint prior of $\boldsymbol{\theta}$, conditional on τ_1, \dots, τ_J , is given by

$$p(\boldsymbol{\theta} | \tau_1, \dots, \tau_J) \propto \exp \left\{ -\frac{1}{2} \boldsymbol{\theta}^\top (\mathbf{D}^\top \mathbf{D} \otimes \text{diag}(\tau_1^{-1}, \dots, \tau_J^{-1})) \boldsymbol{\theta} \right\}.$$

This prior can be interpreted as inducing a second-order random walk process on the sequence of coefficients:

$$\theta_{j,(h)} \sim \mathcal{N}(2\theta_{j,(h-1)} - \theta_{j,(h-2)}, \tau_j), \quad h = 2, 3, \dots, H,$$

given $\theta_{j,(0)}$ and $\theta_{j,(1)}$. The shrinkage parameters were inferred using a half-Cauchy prior with a scale parameter of κ , $\tau_j \sim \mathcal{C}^+(0, \kappa)$. The distribution of τ_j can be represented as follows (Wand et al., 2011; Makalic and Schmidt, 2016):

$$\tau_j | \tilde{\tau}_j \sim \mathcal{IG} \left(\frac{1}{2}, \frac{1}{\tilde{\tau}_j} \right), \quad \tilde{\tau}_j \sim \mathcal{IG} \left(\frac{1}{2}, \frac{1}{\kappa^2} \right),$$

where $\tilde{\tau}_j$ denotes an auxiliary random variable and $\mathcal{IG}(a, b)$ represents an inverse gamma distribution with a shape parameter of a and a rate parameter of b . The conditional posteriors of τ_j and $\tilde{\tau}_j$ are

$$\begin{aligned} \tau_j | \text{rest} &\sim \mathcal{IG} \left(\frac{1}{2} (H - 1), \frac{1}{\tilde{\tau}_j} + \frac{1}{2} \boldsymbol{\theta}_j^\top \mathbf{D}^\top \mathbf{D} \boldsymbol{\theta}_j \right), \\ \tilde{\tau}_j | \text{rest} &\sim \mathcal{IG} \left(1, \frac{1}{\kappa^2} + \frac{1}{\tau_j} \right), \end{aligned}$$

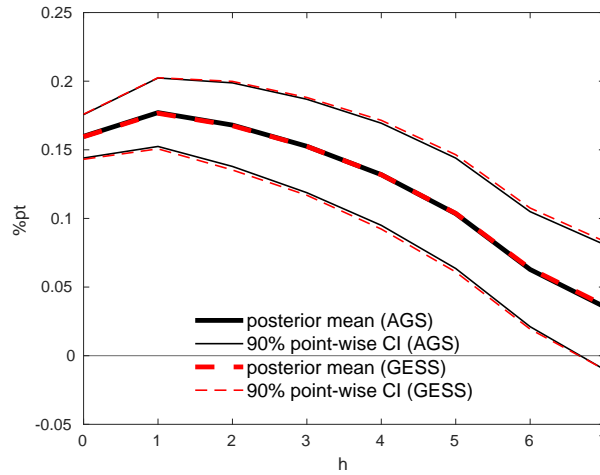
where ‘rest’ denotes the remaining parameters to be sampled. The hyperparameter was set to $\kappa = 100$, making the prior moderately informative. For comparison purposes, we also ran a Gibbs sampler for the pseudo-posterior with the pseudo-likelihood and roughness-penalty prior, where the conditional posterior of $\boldsymbol{\theta}$ was specified as follows:

$$\boldsymbol{\theta} | \text{rest} \sim \mathcal{N}(\mathbf{m}, \mathbf{P}^{-1}),$$

Table 7: Computational efficiency in cases with informative priors

T	Method	minESS/iter	minESS/s
200	Pseudo + Gibbs	.445	509
	LTE + GESS	.001	2
	LTE + AGS	.345	1,008
500	Pseudo + Gibbs	.409	143
	LTE + GESS	.001	1
	LTE + AGS	.364	1,048
1,000	Pseudo + Gibbs	.399	18
	LTE + GESS	.002	1
	LTE + AGS	.377	1,102

Figure 2: Instances of the estimated impulse responses: GESS vs. AGS



$$m = P^{-1} (\Sigma^{-1} \otimes X^T) \text{vec} (Y),$$

$$P = \Sigma^{-1} \otimes X^T X + D^T D \otimes \text{diag} (\tau_1^{-1}, \dots, \tau_J^{-1}).$$

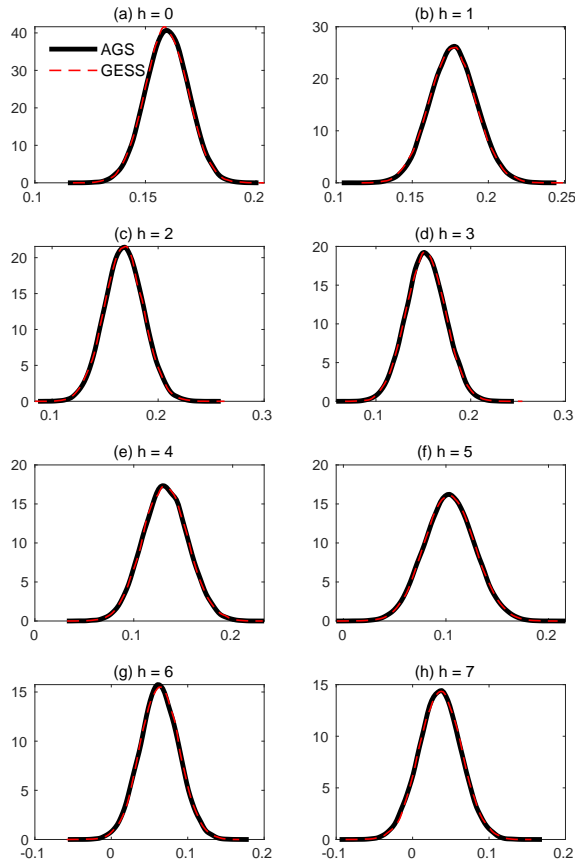
The DGP was the same as before and we used the LD specification.

Table 7 summarizes the computational efficiency measures based on 100 independent runs, each generating 50,000 draws, with the last 40,000 draws used for the analysis. For both minESS/iter and minESS/s, the AGS outperformed the GESS. The GESS exhibited low minESS/iter, reflecting the strong serial correlations in the generated chains. Although the AGS was not particularly efficient, it retained a practical level of efficiency. Regarding minESS/iter, Pseudo with the Gibbs sampler performed comparably to the LTE with the AGS, while minESS/s for Pseudo with the Gibbs sampler was significantly lower than that for the LTE with the AGS. In addition, as the sample size increased, the advantage of the AGS over the Gibbs sampler became more pronounced.

Figure 2 presents an example of the estimated IRFs of interest based on the GESS and AGS, while Figure 3 shows the posterior distributions of the corresponding parameters. Owing to the inefficiency of the GESS, we generated a 20 times longer chain using the GESS to create those figures—specifically, 810,000 draws, using the last 800,000 draws for the evaluation. The GESS and AGS produced nearly identical posterior distributions, suggesting that the AGS can be considered virtually exact.

Figure 4 presents an example of the estimated IRFs of interest based on LTE-raw and Pseudo-

Figure 3: Posterior distributions of the coefficients of interest



sand. These two approaches produced different IRF estimates. However, the difference was not substantial, as the prior was relatively uninformative and the DGP was well behaved, exhibiting a high signal-to-noise ratio. Importantly, these two estimates did not coincide. As demonstrated in Section 4, the discrepancy between these approaches can be significantly larger in real data applications.

3 Extension to the IV Method

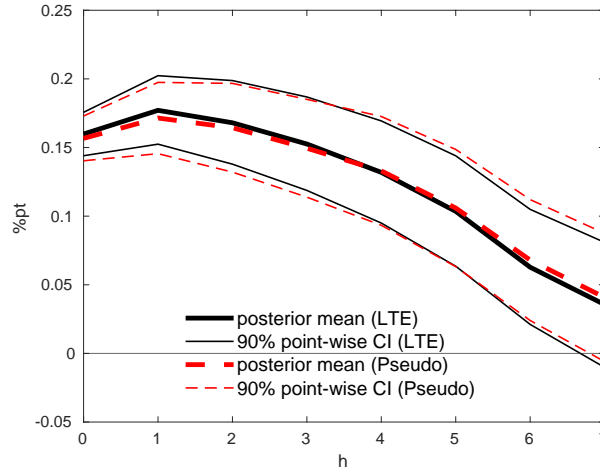
3.1 Quasi-Bayesian LP-IV

Our framework can be naturally extended to IV estimation (Jordà et al., 2015; Ramey, 2016; Stock and Watson, 2018). Let \mathbf{z}_t denote a vector consisting of an IV and exogenous variables, which may overlap with the covariates \mathbf{x}_t . A model of LPs with an IV (i.e., LP-IV) is specified by a set of regression equations as

$$\begin{aligned} x_{1,t} &= g(\mathbf{z}_t) + u_t^\dagger, \\ y_{t+h} &= \boldsymbol{\theta}_{(h)}^\top \mathbf{x}_t + u_{(h),t+h}, \quad h = 0, 1, \dots, H, \end{aligned}$$

where $\boldsymbol{\vartheta}$ denotes a vector of coefficients and u_t^\dagger is an error term. We infer $\boldsymbol{\theta}$ using a set of moment conditions related to the two-stage least squares (TSLS) estimator:

Figure 4: Instances of the estimated impulse responses: LTE vs. Pseudo



$$\mathbf{m}_t(\boldsymbol{\theta}) = \begin{pmatrix} (y_t - \boldsymbol{\theta}_{(0)}^\top \mathbf{x}_t) \mathbf{z}_t \\ (y_{t+1} - \boldsymbol{\theta}_{(1)}^\top \mathbf{x}_t) \mathbf{z}_t \\ \vdots \\ (y_{t+H} - \boldsymbol{\theta}_{(H)}^\top \mathbf{x}_t) \mathbf{z}_t \end{pmatrix}.$$

This approach has two notable features compared with standard Bayesian IV methods such as those of Kleibergen and Zivot (2003); Conley et al. (2008); Lopes and Polson (2014). First, no assumptions are made about the joint distribution of u_t^\dagger and $u_{(0),t}, \dots, u_{(H),t+H}$. Second, there is no need to specify or estimate the first-stage equation explicitly. The weighting matrix is fixed to the inverse of the covariance matrix of the moment function evaluated at the TSLS estimate:

$$\hat{\boldsymbol{\theta}}^{\text{TSLS}} = \text{vec} \left(\left(\hat{\mathbf{X}}^\top \hat{\mathbf{X}} \right)^{-1} \hat{\mathbf{X}}^\top \mathbf{Y} \right),$$

with

$$\hat{\mathbf{X}} = \mathbf{X} \left[(\mathbf{Z}^\top \mathbf{Z})^{-1} \mathbf{Z}^\top \mathbf{X} \right].$$

Posterior simulation for LP-IV is conducted similarly to that for LPs without an IV. The only difference is that we choose $\boldsymbol{\mu} = \hat{\boldsymbol{\theta}}^{\text{TSLS}}$ and $\boldsymbol{\Upsilon} = \mathbf{V} \left(\hat{\boldsymbol{\theta}}^{\text{TSLS}} \right)$.

In this study, we focus solely on the use of external instruments (Stock and Watson, 2012; Mertens and Ravn, 2013). LPs can also be applied with internal instruments, which are obtained by estimating another model such as structural vector autoregressions, as shown by Ramey (2011); Plagborg-Møller and Wolf (2021). However, such a two-step approach does not align with Bayesian analysis, as it ignores the uncertainty surrounding the first-stage estimation.

This study focuses on just-identified cases commonly encountered in the literature. Unlike in LPs without an IV, the number of moment conditions in LP-IV can exceed the number of parameters to be estimated. Although the statistical properties of the LTE in over-identified cases have not been thoroughly investigated, the quasi-posterior for LPs with over-identified moment conditions appears to be not “well calibrated,” as we discuss later.

For point identification, the arguments in the frequentist literature apply (Stock and Watson, 2018; Plagborg-Møller and Wolf, 2021). Suppose y_t is written in terms of current and past structural shocks, $\boldsymbol{\varepsilon}_t = (\varepsilon_{1,t}, \dots, \varepsilon_{M,t})^\top$. Let $\varepsilon_{1,t}$ be the structural shock of interest. Then, we have

$$y_t = \varepsilon_{1,t} + \{\varepsilon_{2:M,t}, \boldsymbol{\varepsilon}_{t-1}, \boldsymbol{\varepsilon}_{t-2}, \dots\},$$

where $\varepsilon_{2:M,t} = (\varepsilon_{2,t}, \dots, \varepsilon_{M,t})^\top$ denotes a vector composed of the structural shocks realized at t except $\varepsilon_{1,t}$ and $\{\cdot\}$ denotes the linear combination operator. For the point identification of the dynamic causal effects, the following three conditions must be met (CONDITION LP-IV in Stock and Watson, 2018):

1. $\mathbb{E} [\varepsilon_{1,t} \mathbf{z}_t] \neq \mathbf{0}$ (relevance);
2. $\mathbb{E} [\varepsilon_{2:M} \mathbf{z}_t^\top] = \mathbf{O}$ (contemporaneous exogeneity);
3. $\mathbb{E} [\varepsilon_{t+j} \mathbf{z}_t^\top] = \mathbf{O}$ for $j \neq 0$ (lead-lag exogeneity),

where \mathbf{O} denotes a matrix of zeros. The first two conditions correspond to those required for conventional IV regression. The third condition requires both that \mathbf{z}_t must be uncorrelated with future shocks and that \mathbf{z}_t must be unpredictable given past shocks. The former is readily satisfied because \mathbf{z}_t is composed of information realized up to the current period, t , and future shocks are unpredictable by definition. By contrast, the latter condition is difficult to meet. To address this issue, we introduce an orthogonalized value by applying a linear projection operator, which is defined for an arbitrary vector \mathbf{a}_t as $\mathbf{a}_t^\perp = \mathbf{a}_t - \text{Proj}(\mathbf{a}_t | \mathbf{x}_t)$. With orthogonalized values, the conditions are modified as follows (CONDITION LP_IV $^\perp$ in Stock and Watson, 2018):

1. $\mathbb{E} [\varepsilon_{1,t}^\perp \mathbf{z}_t^\perp] \neq \mathbf{0}$ (relevance);
2. $\mathbb{E} [\varepsilon_{2:M}^\perp (\mathbf{z}_t^\perp)^\top] = \mathbf{O}$ (contemporaneous exogeneity);
3. $\mathbb{E} [\varepsilon_{t+j}^\perp (\mathbf{z}_t^\perp)^\top] = \mathbf{O}$ for $j \neq 0$ (lead-lag exogeneity).

From a Bayesian perspective, it is recommended to include the lagged exogenous variables into \mathbf{z}_t rather than explicitly estimating the orthogonalized values. Stock and Watson (2018); Rambachan and Shephard (2025) provide a further discussion on the identification of the dynamic causal effects.

3.2 Simulation study

We investigated the frequentist properties of the proposed approach. The DGP was essentially identical to that in Section 2.5. However, because the first variable was not the structural shock, all the entries of Γ_l were filled with non-zero random numbers. A vector of regressors \mathbf{x}_t was similarly defined in the simulation study for LPs without an IV. The vector \mathbf{z}_t was identical to \mathbf{x}_t except that the structural shock (first entry of \mathbf{x}_t) was replaced by an IV, \check{z}_t , which was generated as a noisy observation of the structural shock $\varepsilon_{1,t}$ such that $\check{z}_t = \varepsilon_{1,t} + \epsilon_t$ with $\epsilon_t \sim \mathcal{N}(0, 1)$. We generated 1,000 synthetic datasets.

Tables 8–12 report the results, which were qualitatively similar to those for LPs without an IV. The LD specification exhibited smaller bias than the level specification, particularly when T was small (Table 8). In terms of Bias, the two specifications were comparable (Table 9). When the LD specification was employed, we observed slightly longer Length than with the level specification (Table 10). Finally, the LD specification provided better coverage than the level specification but tended to be overly confident in finite samples (Tables 11 and 12).

To further investigate the finite sample properties of the proposed approach, we conducted additional Monte Carlo experiments that considered more challenging situations such as including a weak instrument, a serially correlated instrument, and many instruments. The DGP of the instruments for $\varepsilon_{1,t}$ was generally specified as

Table 8: Simulation results for LP-IV (1): Median bias

T	Spec.	h							
		0	1	2	3	4	5	6	7
200	Level	.0002	-.0025	-.0042	-.0061	-.0083	-.0091	-.0115	-.0083
	LD	.0003	-.0003	-.0026	-.0042	-.0056	-.0032	-.0013	-.0021
500	Level	-.0004	-.0011	-.0026	-.0029	-.0041	-.0044	-.0038	-.0030
	LD	.0002	-.0001	.0021	-.0023	-.0022	-.0029	-.0038	-.0027
1,000	Level	-.0001	-.0001	-.0004	-.0005	-.0001	-.0008	-.0007	-.0004
	LD	-.0000	-.0000	.0002	-.0009	-.0009	-.0009	-.0004	-.0003

Table 9: Simulation results for LP-IV (2): Median absolute error

T	Spec.	h							
		0	1	2	3	4	5	6	7
200	Level	.005	.015	.022	.025	.028	.028	.029	.030
	LD	.008	.018	.024	.027	.031	.031	.033	.029
500	Level	.004	.010	.014	.017	.018	.018	.019	.018
	LD	.005	.010	.014	.016	.018	.019	.018	.018
1,000	Level	.003	.007	.010	.011	.012	.013	.013	.012
	LD	.003	.008	.010	.011	.013	.014	.014	.013

Table 10: Simulation results for LP-IV (3): Length of the point-wise 90% credible interval

T	Spec.	Cov.	h							
			0	1	2	3	4	5	6	7
200	Level	raw	.023	.062	.092	.110	.120	.124	.126	.127
		sand	.023	.062	.092	.110	.120	.125	.126	.127
	LD	raw	.036	.075	.105	.125	.136	.142	.145	.147
		sand	.036	.075	.105	.125	.136	.142	.145	.147
500	Level	raw	.021	.046	.064	.076	.083	.086	.088	.089
		sand	.021	.046	.064	.076	.083	.086	.088	.089
	LD	raw	.023	.048	.067	.079	.086	.090	.093	.094
		sand	.023	.048	.067	.079	.086	.090	.093	.094
1,000	Level	raw	.012	.031	.044	.053	.057	.060	.061	.062
		sand	.012	.013	.044	.053	.057	.060	.061	.062
	LD	raw	.017	.035	.048	.057	.062	.065	.066	.067
		sand	.017	.035	.048	.057	.062	.065	.066	.067

Table 11: Simulation results for LP-IV (4): Coverage probability of the point-wise 90% credible interval

T	Spec.	Cov.	h							
			0	1	2	3	4	5	6	7
200	Level	raw	.878	.861	.864	.873	.873	.856	.864	.863
		sand	.881	.859	.864	.874	.873	.856	.866	.862
	LD	raw	.893	.873	.860	.869	.891	.883	.885	.904
		sand	.893	.873	.860	.869	.891	.883	.885	.904
500	Level	raw	.889	.891	.873	.883	.886	.890	.884	.887
		sand	.888	.889	.873	.882	.886	.890	.883	.887
	LD	raw	.897	.876	.890	.885	.893	.908	.910	.915
		sand	.898	.878	.890	.886	.893	.908	.910	.914
1,000	Level	raw	.893	.877	.884	.895	.898	.894	.886	.888
		sand	.894	.887	.884	.893	.898	.893	.884	.888
	LD	raw	.906	.878	.875	.881	.890	.881	.881	.893
		sand	.906	.878	.875	.881	.890	.881	.881	.893

Table 12: Simulation results for LP-IV (5): Coverage probability of the simultaneous 90% credible band

T	Spec.	Cov.	plug-in	quantile
200	Level	raw	–	.836
		sand	.864	–
	LD	raw	–	.870
		sand	.870	–
500	Level	raw	–	.873
		sand	.876	–
	LD	raw	–	.893
		sand	.897	–
1,000	Level	raw	–	.875
		sand	.874	–
	LD	raw	–	.883
		sand	.883	–

$$\check{z}_{r,t} = \frac{1}{R}\varepsilon_{1,t} + \rho\frac{1}{R}\check{z}_{1,t} + \sqrt{1-\rho^2}\beta\frac{1}{R}\epsilon_{r,t}, \quad \epsilon_{r,t} \sim \mathcal{N}(0,1), \quad r = 1, \dots, R,$$

where ρ controls the serial correlations in $\check{z}_{r,t}$ and β controls the signal-to-noise ratio. Stacking the equations yields the following representation:

$$\sum_{r=1}^R \check{z}_{r,t} = \varepsilon_{1,t} + \rho\check{z}_{1,t} + \sqrt{1-\rho^2}\beta\frac{1}{R}\sum_{r=1}^R \epsilon_{r,t}.$$

This suggests that regardless of R , a linear combination of the instruments consists of a single instrument with the same ρ and β . The baseline case was that in which $\rho = 0$ (no serial correlation), $\beta = 1$ (low signal-to-noise ratio), and $R = 1$ (single instrument, just-identified). We compared it with alternative cases by varying one parameter as $\rho \in \{0.2, 0.8\}$, $\beta \in \{2, 5\}$, and $R \in \{2, 5, 10\}$ while fixing the others. The sample size was fixed as $T = 500$.

The Online Appendix reports the results. Tables A.3–A.7 summarize the results for different β values with weak instruments. When the instrument was moderately weak ($\beta = 2$), the frequentist properties were only slightly affected. However, when the instrument was very weak ($\beta = 5$), the situation worsened. In particular, as the instruments became weaker, Length tended to rise (Table A.5) and both P-Coverage and S-Coverage tended to exceed the nominal level (Tables A.6 and A.7). This suggests the importance of using a strong instrument in practice and highlights the need to develop a tool to detect and address weak instruments. Tables A.8–A.12 present the results for different ρ values, reflecting the serial correlations in the instrument. The increase in serial correlations did not significantly affect the frequentist properties of the proposed approach. Therefore, as long as the lagged variables are included in \mathbf{x}_t and \mathbf{z}_t , the approach appears to be robust to the serial correlations in an IV. Tables A.13–A.17 present the results for different R values, reflecting the number of instruments. Using several weak instruments ($R = 2$ or $R = 5$) improved the performance of the point estimation compared with $R = 1$, while using many weak instruments ($R = 10$) worsened it (Tables A.13 and A.14). The main issue with using multiple IVs is that the nominal coverage is likely to deviate significantly from the desired level: as R increases, P-Coverage and S-Coverage decreased, moving further from the target of 90% (Tables A.16 and A.17).

4 Application to Real Data

To demonstrate its real-world application, we applied the proposed approach to analyze U.S. monetary policy. We used three sets of time series data retrieved from the FRED database:¹¹ the monthly growth rate of the industrial production index ΔIP_t (FRED mnemonic: INDPRO), the monthly growth rate of the consumer price index ΔCPI_t (CPIAUCSL), and the interest rate on one-year U.S. Treasury bonds R_t (GS1). In addition, we used Gilchrist and Zakrajšek's (2012) excess bond premium GZ_t as an indicator of financial stress.¹² As the IV for R_t , we used high-frequency U.S. monetary policy surprises MPS_t (Swanson and Jayawickrema, 2024).¹³ The macroeconomic indicators ΔIP_t and ΔCPI_t were multiplied by 100 so that they were measured in percentage point growth rates. The financial market indicators R_t and GZ_t were measured in percentage points at the annual rate. The raw data spanned 1988:2 to 2023:12

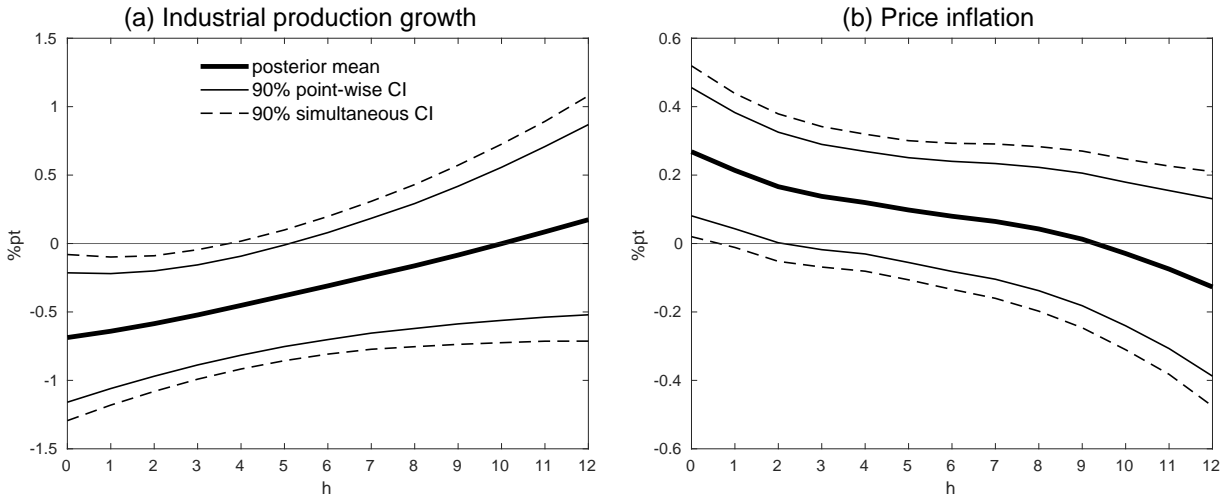
¹¹<https://fred.stlouisfed.org/>.

¹²We used the 2023 update (Favara et al., 2016).

¹³<https://www.frbsf.org/research-and-insights/data-and-indicators/monetary-policy-surprises/>.

¹⁴See also Bauer and Swanson (2023); Swanson (2023).

Figure 5: Estimated impulse responses



Note: The bold solid lines indicate the posterior means. The thin solid lines indicate the point-wise 90% credible intervals. The thin dashed lines indicate the simultaneous 90% credible bands.

owing to the availability of data on monetary policy surprises. We considered the response up to $H = 12$ horizons. The regressor x_t included the treatment R_t , an intercept, and up to $L = 4$ lags of the four variables, $\Delta IP_t, \Delta CPI_t, R_t, GZ_t$. We employed the LD specification, and the lags of ΔIP_t (ΔCPI_t) were replaced by the lags of its first difference when ΔIP_t (ΔCPI_t) was the response variable. The vector z_t was identical to x_t but the first entry was replaced by the IV MPS_t . The effective time series length was $T = 413$ and the number of unknown parameters was $D = (2 + 4L)(H + 1) = 234$. The prior specification was the same as that in Section 2.5. We generated 40,000 posterior draws after discarding 10,000 draws as the burn-in.

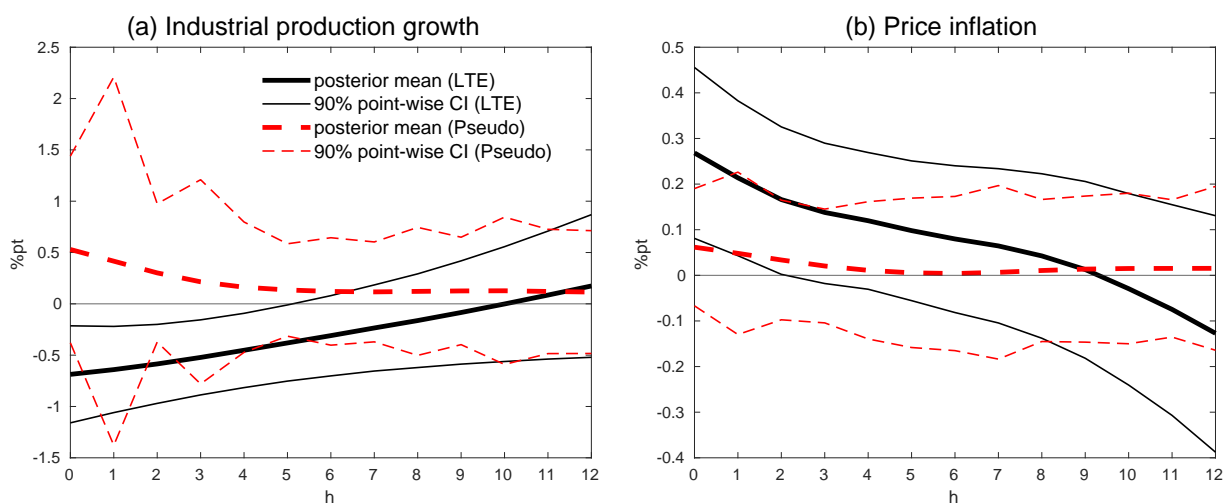
Figure 5 plots the posterior mean estimates of the impulse responses along with the corresponding point-wise 90% credible intervals and simultaneous 90% credible bands. Panel (a) presents the results for industrial production growth, while Panel (b) shows the results for inflation. In both cases, the simultaneous credible bands are noticeably wider than the point-wise credible intervals. This highlights the practical importance of estimating simultaneous credible bands, which cannot be achieved using Ferreira et al.’s (forthcoming) approach.

Figure 6 presents the estimated impulse responses using Pseudo-sand and LTE-raw, which differed drastically. In applications of LPs, sample sizes are typically small relative to the number of unknown parameters—this is especially true for the simultaneous inference of LPs, as in this study. Consequently, prior specification can significantly influence the posterior distribution of LP coefficients. It is crucial for analysts to select a scientifically appropriate prior—not only allowing the data to speak but also ensuring that prior elicitation is carefully considered. In this regard, the proposed approach, which produces a “well calibrated” posterior, can serve as a valuable scientific tool for LP analysis.

5 Conclusion

In this study, we introduced a novel quasi-Bayesian approach for inferring LPs. The proposed approach offers three key advantages over those presented in previous studies. First, the quasi-posterior, based on a GMM criterion, is “well calibrated” compared with the posterior based

Figure 6: Estimated impulse responses



Note: The bold lines indicate the posterior means. The thin lines indicate the point-wise 90% credible intervals. The black solid lines indicate the results for LTE-raw. The red dashed lines indicate the results for Pseudo-sand.

on the pseudo-likelihood in that its credible intervals closely align with their asymptotic counterparts. This ensures a proper balance between the likelihood and prior in posterior estimation. Second, our approach facilitates the estimation of simultaneous credible bands. Third, it naturally accommodates IV estimation. While there are frequentist contributions in both methodology and application, this is the first study to infer LP-IV within a Bayesian framework. Additionally, we developed practical posterior simulators based on the GESS and AGS and demonstrated the effectiveness of our approach through extensive Monte Carlo simulations as well as an empirical application to U.S. monetary policy. These contributions have broad implications for applied macroeconomics and econometrics, where LPs are increasingly used to study dynamic causal effects. This research aims to encourage further methodological development and application.

Many research issues remain to be addressed. The proposed LP-IV approach does not explicitly estimate the first-stage equation, which has both advantages and disadvantages. On the one hand, using this approach mitigates the misspecification problem (e.g., the functional form of the first-stage equation and joint distribution of the error terms) and eliminates the need to infer auxiliary unknown parameters, which are rarely of primary interest. On the other hand, adopting this approach presents hurdles when dealing with many and/or weak instruments. In Bayesian IV regression, shrinkage priors are commonly used to address the problem of many and/or weak instruments (Wiesenfarth et al., 2014; Hahn et al., 2018; Kato and Hoshino, 2021). However, these priors cannot be applied in our context. While many frequentist solutions to the many and/or weak instruments problem have been proposed,¹⁵ adapting these methods to a Bayesian framework appears challenging. Therefore, methods to address the many and/or weak instruments problem within the quasi-Bayesian LPs framework must be urgently developed. Theoretical investigations and the development of solutions for the LTE in the case of over-identification are also needed, although this is an issue not only for LPs but also more generally. Additionally, the proposed approach could be extended in several potential directions using in-

¹⁵See Andrews et al. (2019); Keane and Neal (2024) for a recent review.

verse propensity scores (Jordà and Taylor, 2016; Angrist et al., 2018), panel data (Dube et al., 2023; de Chaisemartin and d’Haultfoeuille, forthcoming), and multiple responses (Aruoba and Drechsel, 2024).

References

- Andrews, Isaiah, James H. Stock, and Liyang Sun (2019) “Weak Instruments in Instrumental Variables Regression: Theory and Practice,” *Annual Review of Economics*, 11 (1), 727–753.
- Angrist, Joshua D., Òscar Jordà, and Guido M. Kuersteiner (2018) “Semiparametric Estimates of Monetary Policy Effects: String Theory Revisited,” *Journal of Business and Economic Statistics*, 36 (3), 371–387.
- Aruoba, S. Borağan and Thomas Drechsel (2024) “The Long and Variable Lags of Monetary Policy: Evidence from Disaggregated Price Indices,” *Journal of Monetary Economics*, 148, 103635.
- Bauer, Michael D. and Eric T. Swanson (2023) “A Reassessment of Monetary Policy Surprises and High-Frequency Identification,” *NBER Macroeconomics Annual*, 37 (1), 87–155.
- Brignone, Riccardo, Luca Gonzato, and Eva Lütkebohmert (2023) “Efficient Quasi-Bayesian Estimation of Affine Option Pricing Models Using Risk-neutral Cumulants,” *Journal of Banking and Finance*, 148, 106745.
- Brugnolini, Luca, Leopoldo Catania, Pernille Hansen, and Paolo Santucci de Magistris (2024) “Bayesian Flexible Local Projections,” *Studies in Nonlinear Dynamics & Econometrics*, 28 (2), 435–462.
- Cabezas, Alberto and Christopher Nemeth (2023) “Transport Elliptical Slice Sampling,” in *Proceedings of the 26th International Conference on Artificial Intelligence and Statistics (AISTATS) 2023*, 3664–3676, PMLR.
- Chernozhukov, Victor and Han Hong (2003) “An MCMC Approach to Classical Estimation,” *Journal of Econometrics*, 115 (2), 293–346.
- Conley, Timothy G., Christian B. Hansen, Robert E. McCulloch, and Peter E. Rossi (2008) “A Semi-parametric Bayesian Approach to the Instrumental Variable Problem,” *Journal of Econometrics*, 144 (1), 276–305.
- de Chaisemartin, Clément and Xavier d’Haultfoeuille (forthcoming) “Difference-in-differences Estimators of Intertemporal Treatment Effects,” *Review of Economics and Statistics*.
- Dube, Arindrajit, Daniele Girardi, Òscar Jordà, and Alan M. Taylor (2023) “A Local Projections Approach to Difference-in-Differences Event Studies,” Technical report, National Bureau of Economic Research Working Paper 31184.
- El-Shagi, Makram (2019) “A Simple Estimator for Smooth Local Projections,” *Applied Economics Letters*, 26 (10), 830–834.

- Favara, Giovanni, Simon Gilchrist, Kurt F. Lewis, and Egon Zakrajšek (2016) “Updating the Recession Risk and the Excess Bond Premium,” Technical report, FEDS Notes. Washington: Board of Governors of the Federal Reserve System, October 6, 2016, <https://doi.org/10.17016/2380-7172.1836>.
- Ferreira, Leonardo N., Silvia Miranda-Agrippino, and Giovanni Ricco (forthcoming) “Bayesian Local Projections,” *Review of Economics and Statistics*.
- Gilchrist, Simon and Egon Zakrajšek (2012) “Credit Spreads and Business Cycle Fluctuations,” *American Economic Review*, 102 (4), 1692–1720.
- Hahn, P. Richard, Jingyu He, and Hedibert Lopes (2018) “Bayesian Factor Model Shrinkage for Linear IV Regression with Many Instruments,” *Journal of Business and Economic Statistics*, 36 (2), 278–287.
- Hahn, P. Richard, Jingyu He, and Hedibert F. Lopes (2019) “Efficient Sampling for Gaussian Linear Regression with Arbitrary Priors,” *Journal of Computational and Graphical Statistics*, 28 (1), 142–154.
- Hansen, Lars Peter (1982) “Large Sample Properties of Generalized Method of Moments Estimators,” *Econometrica*, 50 (4), 1029–1054.
- Herbst, Edward P. and Benjamin K. Johansson (2024) “Bias in Local Projections,” *Journal of Econometrics*, 240 (1), 105655.
- Hong, Han, Huiyu Li, and Jessie Li (2021) “BLP Estimation Using Laplace Transformation and Overlapping Simulation Draws,” *Journal of Econometrics*, 222 (1), 56–72.
- Huber, Florian, Christian Matthes, and Michael Pfarrhofer (2024) “General Seemingly Unrelated Local Projections,” Technical report, arXiv preprint, arXiv:2410.17105.
- Jordà, Òscar (2005) “Estimation and Inference of Impulse Responses Local Projections,” *American Economic Review*, 95 (1), 161–182.
- (2009) “Simultaneous Confidence Regions for Impulse Responses,” *Review of Economics and Statistics*, 91 (3), 629–647.
- (2023) “Local Projections for Applied Economics,” *Annual Review of Economics*, 15 (1), 607–631.
- Jordà, Òscar, Moritz Schularick, and Alan M. Taylor (2015) “Betting the House,” *Journal of International Economics*, 96, S2–S18.
- (2020) “The Effects of Quasi-random Monetary Experiments,” *Journal of Monetary Economics*, 112, 22–40.
- Jordà, Òscar, Sanjay R. Singh, and Alan M. Taylor (forthcoming) “The Long-run Effects of Monetary Policy,” *Review of Economics and Statistics*.
- Jordà, Òscar and Alan M. Taylor (2016) “The Time for Austerity: Estimating the Average Treatment Effect of Fiscal Policy,” *Economic Journal*, 126 (590), 219–255.
- (2024) “Local Projections,” Technical report, NBER Working Paper 32822.

- Kato, Ryo and Takahiro Hoshino (2021) “Semiparametric Bayes Instrumental Variable Estimation with Many Weak Instruments,” *Stat*, 10 (1), e350.
- Keane, Michael P. and Timothy Neal (2024) “A Practical Guide to Weak Instruments,” *Annual Review of Economics*, 16.
- Kilian, Lutz (1998) “Small-sample Confidence Intervals for Impulse Response Functions,” *Review of Economics and Statistics*, 80 (2), 218–230.
- Kim, Jae-Young (2002) “Limited Information Likelihood and Bayesian Analysis,” *Journal of Econometrics*, 107 (1-2), 175–193.
- Kleibergen, Frank and Eric Zivot (2003) “Bayesian and Classical Approaches to Instrumental Variable Regression,” *Journal of Econometrics*, 114 (1), 29–72.
- Kormilitsina, Anna and Denis Nekipelov (2016) “Consistent Variance of the Laplace-type Estimators: Application to DSGE Models,” *International Economic Review*, 57 (2), 603–622.
- Lazarus, Eben, Daniel J. Lewis, James H. Stock, and Mark W. Watson (2018) “HAR Inference: Recommendations for Practice,” *Journal of Business and Economic Statistics*, 36 (4), 541–559.
- Li, Dake, Mikkel Plagborg-Møller, and Christian K. Wolf (2024) “Local Projections vs. VARs: Lessons from Thousands of DGPs,” *Journal of Econometrics*, 244 (2), 105722.
- Lopes, Hedibert F. and Nicholas G. Polson (2014) “Bayesian Instrumental Variables: Priors and Likelihoods,” *Econometric Reviews*, 33 (1-4), 100–121.
- Makalic, Enes and Daniel F. Schmidt (2016) “A Simple Sampler for the Horseshoe Estimator,” *IEEE Signal Processing Letters*, 23 (1), 179–182.
- Martin, Ryan and Nicholas Syring (2022) “Direct Gibbs Posterior Inference on Risk Minimizers: Construction, Concentration, and Calibration,” in *Handbook of Statistics*, 47, 1–41: Elsevier.
- Mertens, Karel and José Luis Montiel Olea (2018) “Marginal Tax Rates and Income: New Time Series Evidence,” *Quarterly Journal of Economics*, 133 (4), 1803–1884.
- Mertens, Karel and Morten O. Ravn (2013) “The Dynamic Effects of Personal and Corporate Income Tax Changes in the United States,” *American Economic Review*, 103 (4), 1212–1247.
- Montiel Olea, José Luis and Mikkel Plagborg-Møller (2019) “Simultaneous Confidence Bands: Theory, Implementation, and an Application to SVARs,” *Journal of Applied Econometrics*, 34 (1), 1–17.
- (2021) “Local Projection Inference Is Simpler and More Robust Than You Think,” *Econometrica*, 89 (4), 1789–1823.
- Müller, Ulrich K. (2013) “Risk of Bayesian Inference in Misspecified Models, and the Sandwich Covariance Matrix,” *Econometrica*, 81 (5), 1805–1849.
- Murray, Iain, Ryan Adams, and David MacKay (2010) “Elliptical Slice Sampling,” in *Proceedings of the 13th International Conference on Artificial Intelligence and Statistics*, 541–548, JMLR Workshop and Conference Proceedings.

- Nesterov, Yurii (2009) “Primal-dual subgradient methods for convex problems,” *Mathematical Programming*, 120 (1), 221–259.
- Newey, Whitney K. and Kenneth D. West (1987) “A Simple, Positive Semi-definite, Heteroskedasticity and Autocorrelation Consistent Covariance Matrix,” *Econometrica*, 55 (3), 703–08.
- Nishihara, Robert, Iain Murray, and Ryan P. Adams (2014) “Parallel MCMC with Generalized Elliptical Slice Sampling,” *Journal of Machine Learning Research*, 15 (1), 2087–2112.
- Piger, Jeremy and Thomas Stockwell (2025) “Differences from Differencing: Should Local Projections with Observed Shocks Be Estimated in Levels or Differences?” Technical report, Available at SSRN: <https://ssrn.com/abstract=4530799> or <http://dx.doi.org/10.2139/ssrn.4530799>.
- Plagborg-Møller, Mikkel and Christian K. Wolf (2021) “Local Projections and Vars Estimate the Same Impulse Responses,” *Econometrica*, 89 (2), 955–980.
- (2022) “Instrumental Variable Identification of Dynamic Variance Decompositions,” *Journal of Political Economy*, 130 (8), 2164–2202.
- Rambachan, Ashesh and Neil Shephard (2025) “When Do Common Time Series Estimands Have Nonparametric Causal Meaning?” Technical report, arXiv preprint, arXiv:1903.01637.
- Ramey, Valere A. (2016) “Macroeconomic Shocks and Their Propagation,” in Taylor, John B. and Harald Uhlig eds. *Handbook of Macroeconomics*, 2A, Chap. 2, 71–162: Elsevier.
- Ramey, Valerie A. (2011) “Identifying Government Spending Shocks: It’s All in the Timing,” *Quarterly Journal of Economics*, 126 (1), 1–50.
- Ramey, Valerie A. and Sarah Zubairy (2018) “Government Spending Multipliers in Good Times and in Bad: Evidence from US Historical Data,” *Journal of Political Economy*, 126 (2), 850–901.
- Roberts, G.O., A. Gelman, and W.R. Gilks (1997) “Weak Convergence and Optimal Scaling of Random Walk Metropolis Algorithms,” *Annals of Applied Probability*, 7 (1), 110–120.
- Rue, Håvard (2001) “Fast Sampling of Gaussian Markov Random Fields,” *Journal of the Royal Statistical Society, Series B*, 63 (2), 325–338.
- Stock, James H. and Mark W. Watson (2012) “Disentangling the Channels of the 2007–09 Recession,” *Brookings Papers on Economic Activity*, 2012 (1), 81–135.
- (2018) “Identification and Estimation of Dynamic Causal Effects in Macroeconomics Using External Instruments,” *Economic Journal*, 128 (610), 917–948.
- Swanson, Eric T. (2023) “The Importance of Fed Chair Speeches As a Monetary Policy Tool,” in *AEA Papers and Proceedings*, 113, 394–400.
- Swanson, Eric T. and Vishuddhi Jayawickrema (2024) “Speeches by the Fed Chair Are More Important Than FOMC Announcements: An Improved High-Frequency Measure of U.S. Monetary Policy Shocks,” Technical report, University of California, Irvine.

- Tanaka, Masahiro (2018) “Adaptive MCMC for Generalized Method of Moments with Many Moment Conditions,” Technical report, arXiv preprint arXiv:1811.00722.
- (2020a) “Bayesian Inference of Local Projections with Roughness Penalty Priors,” *Computational Economics*, 55 (2), 629–651.
- (2020b) “On the Likelihood of Local Projection Models,” Technical report, arXiv preprint, arXiv:2005.12620.
- Walker, Stephen G. (2013) “Bayesian Inference with Misspecified Models,” *Journal of Statistical Planning and Inference*, 143 (10), 1621–1633.
- Wand, Matthew P., John T. Ormerod, Simone A. Padoan, and Rudolf Frühwirth (2011) “Mean Field Variational Bayes for Elaborate Distributions,” *Bayesian Analysis*, 6 (4), 847–900.
- Wiesenfarth, Manuel, Carlos Matías Hisgen, Thomas Kneib, and Carmen Cadarso-Suarez (2014) “Bayesian Nonparametric Instrumental Variables Regression Based on Penalized Splines and Dirichlet Process Mixtures,” *Journal of Business and Economic Statistics*, 32 (3), 468–482.
- Wu, Pei-Shien and Ryan Martin (2023) “A Comparison of Learning Rate Selection Methods in Generalized Bayesian Inference,” *Bayesian Analysis*, 18 (1), 105–132.
- Yin, Guosheng (2009) “Bayesian Generalized Method of Moments,” *Bayesian Analysis*, 4 (2), 191–208.
- Yin, Guosheng, Yanyuan Ma, Faming Liang, and Ying Yuan (2011) “Stochastic Generalized Method of Moments,” *Journal of Computational and Graphical Statistics*, 20 (3), 714–727.
- Zellner, Arnold (1962) “An Efficient Method of Estimating Seemingly Unrelated Regressions and Tests for Aggregation Bias,” *Journal of the American Statistical Association*, 57 (298), 348–368.

Online Appendix for “Quasi-Bayesian Local Projections: Simultaneous Inference and Extension to Instrumental Variable Method”

Masahiro Tanaka*

March 26, 2025

*Faculty of Economics, Fukuoka University, Fukuoka, Japan. Address: 8-19-1, Nanakuma, Jonan, Fukuoka, Japan 814-0180. E-mail: gspddlnt45@toki.waseda.jp.

Table A.1: Simulation result for LPs : Coverage probability of point-wise 90% credible interval

T	Spec.	Method	Cov.	h								
				0	1	2	3	4	5	6	7	
200	Level	Pseudo	HAR	sand	.840	.816	.814	.803	.806	.785	.812	.798
				raw	.870	.849	.854	.842	.825	.836	.843	.846
		LTE	plain	sand	.869	.849	.858	.844	.825	.834	.846	.847
				raw	.840	.816	.815	.802	.810	.788	.811	.797
		HAR	sand	raw	.839	.817	.815	.802	.808	.788	.815	.797
				sand	.826	.823	.846	.830	.831	.833	.819	.839
	LD	Pseudo	HAR	sand	.826	.823	.846	.830	.831	.833	.819	.839
				raw	.868	.871	.875	.878	.879	.870	.862	.865
		LTE	plain	sand	.869	.870	.874	.878	.878	.870	.862	.866
				raw	.824	.822	.841	.829	.834	.834	.820	.834
		HAR	sand	raw	.825	.822	.842	.830	.832	.834	.822	.837
				sand	.870	.857	.875	.849	.854	.852	.849	.845
500	Level	Pseudo	HAR	sand	.870	.857	.875	.849	.854	.852	.849	.845
				raw	.895	.881	.890	.885	.887	.887	.877	.889
		LTE	plain	sand	.896	.879	.891	.885	.890	.885	.875	.888
				raw	.871	.859	.871	.849	.853	.847	.849	.845
		HAR	sand	raw	.870	.858	.873	.849	.854	.849	.850	.846
				sand	.881	.869	.873	.875	.880	.878	.865	.861
	LD	Pseudo	HAR	sand	.881	.869	.873	.875	.880	.878	.865	.861
				raw	.895	.893	.902	.896	.903	.904	.893	.892
		LTE	plain	sand	.894	.891	.903	.896	.904	.903	.893	.896
				raw	.882	.867	.876	.873	.880	.877	.864	.859
		HAR	sand	raw	.884	.869	.874	.874	.879	.878	.865	.860
				sand	.880	.866	.864	.858	.841	.847	.848	.859
1,000	Level	Pseudo	HAR	sand	.880	.866	.864	.858	.841	.847	.848	.859
				raw	.896	.885	.874	.883	.873	.875	.878	.887
		LTE	plain	sand	.896	.885	.875	.885	.876	.877	.879	.885
				raw	.879	.864	.864	.857	.845	.845	.850	.858
		HAR	sand	raw	.878	.865	.864	.856	.843	.847	.847	.858
				sand	.894	.887	.879	.881	.876	.873	.888	.878
	LD	Pseudo	HAR	sand	.894	.887	.879	.881	.876	.873	.888	.878
				raw	.903	.902	.891	.898	.894	.892	.907	.901
		LTE	plain	sand	.904	.904	.891	.898	.895	.890	.908	.901
				raw	.890	.889	.878	.883	.877	.873	.887	.877
		HAR	sand	raw	.892	.889	.878	.880	.876	.873	.888	.877
				sand	.892	.889	.878	.880	.876	.873	.888	.877

Table A.2: Simulation result for LPs : Coverage probability of simultaneous 90% credible band

T	Spec.	Cov.		plug-in	quantile
200	Level	plain	raw	–	.835
			sand	.831	–
	HAR	raw	sand	–	.693
			sand	.699	–
	LD	plain	raw	–	.840
			sand	.842	–
HAR	raw	sand	–	.737	
		sand	.730	–	
500	Level	plain	raw	–	.890
			sand	.891	–
	HAR	raw	sand	–	.805
			sand	.804	–
	LD	plain	raw	–	.890
			sand	.892	–
HAR	raw	sand	–	.831	
		sand	.829	–	
1,000	Level	plain	raw	–	.863
			sand	.864	–
	HAR	raw	sand	–	.805
			sand	.808	–
	LD	plain	raw	–	.892
			sand	.892	–
HAR	raw	sand	–	.857	
		sand	.857	–	

Table A.3: Simulation result for LP-IV (1): Median bias

β	Spec.	h							
		0	1	2	3	4	5	6	7
1	Level	-.0004	-.0011	-.0026	-.0029	-.0041	-.0044	-.0038	-.0030
	LD	-.0002	-.0008	-.0021	-.0023	-.0022	-.0029	-.0038	-.0027
2	Level	.0003	.0006	.0010	.0013	-.0002	-.0016	-.0029	-.0041
	LD	.0001	-.0003	-.0020	-.0015	-.0014	-.0021	-.0018	-.0016
5	Level	.0009	-.0019	-.0082	-.0048	-.0069	-.0053	.0031	-.0005
	LD	.0041	.0035	.0056	.0009	.0007	-.0016	.0003	.0019

Table A.4: Simulation result for LP-IV (2): Median absolute error

β	Spec.	h							
		0	1	2	3	4	5	6	7
1	Level	.004	.010	.014	.017	.018	.018	.019	.018
	LD	.005	.010	.014	.016	.018	.019	.018	.018
2	Level	.007	.016	.022	.027	.029	.030	.031	.031
	LD	.008	.017	.024	.028	.029	.032	.031	.031
5	Level	.030	.052	.060	.068	.075	.081	.079	.090
	LD	.032	.048	.063	.074	.080	.083	.078	.080

Table A.5: Simulation result for LP-IV (3): Length of point-wise 90% credible interval

β	Spec.	Cov.	h							
			0	1	2	3	4	5	6	7
1	Level	raw	.021	.046	.064	.076	.083	.086	.088	.089
		sand	.021	.046	.064	.076	.083	.086	.088	.089
	LD	raw	.023	.048	.067	.079	.086	.090	.093	.094
		sand	.023	.048	.067	.079	.086	.090	.093	.094
2	Level	raw	.033	.074	.105	.125	.135	.141	.144	.146
		sand	.038	.077	.107	.126	.137	.143	.146	.148
	LD	raw	.038	.077	.107	.126	.137	.143	.146	.148
		sand	.038	.077	.107	.126	.137	.143	.146	.148
5	Level	raw	.140	.233	.303	.347	.373	.389	.398	.400
		sand	.140	.232	.303	.347	.374	.388	.397	.400
	LD	raw	.145	.238	.314	.365	.396	.412	.418	.420
		sand	.145	.238	.314	.366	.395	.412	.419	.420

Table A.6: Simulation result for LP-IV (4): Coverage probability of point-wise 90% credible interval

β	Spec.	Cov.	h							
			0	1	2	3	4	5	6	7
1	Level	raw	.889	.891	.873	.883	.886	.890	.884	.887
		sand	.888	.889	.873	.882	.886	.890	.883	.887
	LD	raw	.897	.876	.890	.885	.893	.908	.910	.915
		sand	.898	.878	.890	.886	.893	.908	.911	.914
2	Level	raw	.893	.884	.883	.891	.873	.882	.892	.877
		sand	.892	.883	.885	.891	.874	.882	.893	.877
	LD	raw	.891	.881	.876	.872	.866	.880	.876	.907
		sand	.889	.881	.874	.872	.866	.881	.876	.908
5	Level	raw	.919	.915	.926	.931	.922	.919	.912	.913
		sand	.917	.912	.926	.930	.920	.918	.911	.911
	LD	raw	.926	.919	.935	.925	.919	.909	.913	.916
		sand	.925	.919	.936	.924	.920	.910	.914	.918

Table A.7: Simulation result for LP-IV (5): Coverage probability of simultaneous 90% credible band

β	Spec.	Cov.	plug-in	quantile
1	Level	raw	–	.873
		sand	.876	–
	LD	raw	–	.893
		sand	.897	–
2	Level	raw	–	.889
		sand	.888	–
	LD	raw	–	.891
		sand	.889	–
5	Level	raw	–	.959
		sand	.961	–
	LD	raw	–	.951
		sand	.953	–

Table A.8: Simulation result for LP-IV (1): Median bias

ρ	Spec.	h							
		0	1	2	3	4	5	6	7
0.0	Level	-.0004	-.0011	-.0026	-.0029	-.0041	-.0044	-.0038	-.0030
	LD	-.0002	-.0008	-.0021	-.0023	-.0022	-.0029	-.0038	-.0027
0.2	Level	-.0002	-.0006	-.0017	-.0028	-.0025	-.0035	-.0029	-.0015
	LD	.0000	-.0006	-.0015	-.0015	-.0023	-.0017	-.0024	-.0009
0.8	Level	-.0002	-.0005	-.0013	-.0024	-.0023	-.0031	-.0023	-.0021
	LD	.0001	-.0000	.0002	-.0009	-.0011	-.0020	-.0020	-.0021

Table A.9: Simulation result for LP-IV (2): Median absolute error

ρ	Spec.	h							
		0	1	2	3	4	5	6	7
0.0	Level	.004	.010	.014	.017	.018	.018	.019	.018
	LD	.005	.010	.014	.016	.018	.019	.018	.018
0.2	Level	.003	.008	.013	.015	.016	.017	.018	.018
	LD	.004	.009	.013	.014	.018	.018	.019	.019
0.8	Level	.002	.007	.010	.013	.014	.015	.014	.014
	LD	.002	.007	.010	.012	.015	.015	.015	.015

Table A.10: Simulation result for LP-IV (3): Length of point-wise 90% credible interval

ρ	Spec.	Cov.	h							
			0	1	2	3	4	5	6	7
0.0	Level	raw	.021	.046	.064	.076	.083	.086	.088	.089
		sand	.021	.046	.064	.076	.083	.086	.088	.089
	LD	raw	.023	.048	.067	.079	.086	.090	.093	.094
		sand	.023	.048	.067	.079	.086	.090	.093	.094
0.2	Level	raw	.016	.040	.059	.070	.077	.080	.082	.083
		sand	.016	.040	.059	.071	.077	.080	.082	.083
	LD	raw	.017	.041	.061	.073	.080	.084	.086	.087
		sand	.017	.041	.061	.073	.080	.084	.086	.087
0.8	Level	raw	.009	.031	.047	.057	.063	.065	.067	.067
		sand	.009	.031	.047	.057	.063	.065	.067	.068
	LD	raw	.011	.032	.048	.058	.064	.066	.068	.069
		sand	.011	.032	.048	.058	.064	.067	.068	.069

Table A.11: Simulation result for LP-IV (4): Coverage probability of point-wise 90% credible interval

ρ	Spec.	Cov.	h							
			0	1	2	3	4	5	6	7
0.0	Level	raw	.889	.891	.873	.883	.886	.890	.884	.887
		sand	.888	.889	.873	.882	.886	.890	.883	.887
	LD	raw	.897	.876	.890	.885	.893	.908	.910	.915
		sand	.898	.878	.890	.886	.893	.908	.911	.914
0.2	Level	raw	.886	.889	.889	.886	.887	.881	.876	.884
		sand	.886	.889	.888	.886	.886	.881	.879	.885
	LD	raw	.904	.916	.905	.891	.869	.876	.868	.885
		sand	.903	.916	.904	.895	.870	.875	.871	.883
0.8	Level	raw	.895	.894	.878	.868	.862	.888	.881	.907
		sand	.896	.893	.878	.869	.863	.887	.877	.905
	LD	raw	.892	.900	.883	.886	.870	.865	.871	.875
		sand	.894	.900	.881	.885	.870	.867	.871	.876

Table A.12: Simulation result for LP-IV (5): Coverage probability of simultaneous 90% credible band

ρ	Spec.	Cov.	plug-in	quantile
0.0	Level	raw	–	.873
		sand	.876	–
	LD	raw	–	.893
		sand	.897	–
0.2	Level	raw	–	.863
		sand	.862	–
	LD	raw	–	.881
		sand	.881	–
0.8	Level	raw	–	.875
		sand	.874	–
	LD	raw	–	.879
		sand	.876	–

Table A.13: Simulation result for LP-IV (1): Median bias

R	Spec.	h							
		0	1	2	3	4	5	6	7
1	Level	-.0004	-.0011	-.0026	-.0029	-.0041	-.0044	-.0038	-.0030
	LD	-.0002	-.0008	-.0021	-.0023	-.0022	-.0029	-.0038	-.0027
2	Level	-.0002	-.0013	-.0023	-.0032	-.0044	-.0048	-.0046	-.0043
	LD	-.0001	-.0005	-.0014	-.0015	-.0018	-.0015	-.0028	-.0018
5	Level	.0000	-.0005	-.0011	-.0009	-.0021	-.0029	-.0037	-.0033
	LD	.0004	-.0001	-.0004	-.0013	-.0009	-.0006	-.0003	-.0017
10	Level	.0005	-.0005	-.0010	-.0025	-.0018	-.0019	-.0036	-.0011
	LD	.0003	-.0002	.0013	.0012	-.0001	-.0009	-.0008	-.0010

Table A.14: Simulation result for LP-IV (2): Median absolute error

R	Spec.	h							
		0	1	2	3	4	5	6	7
1	Level	.004	.010	.014	.017	.018	.018	.019	.018
	LD	.005	.010	.014	.016	.018	.019	.018	.018
2	Level	.001	.006	.009	.011	.012	.013	.013	.013
	LD	.001	.006	.009	.011	.011	.012	.012	.012
5	Level	.004	.007	.011	.013	.013	.014	.014	.014
	LD	.004	.008	.011	.013	.014	.015	.015	.016
10	Level	.008	.012	.016	.018	.020	.019	.020	.021
	LD	.008	.013	.017	.019	.020	.022	.023	.021

Table A.15: Simulation result for LP-IV (3): Length of point-wise 90% credible interval

R	Spec.	Cov.	h							
			0	1	2	3	4	5	6	7
1	Level	raw	.021	.046	.064	.076	.083	.086	.088	.089
		sand	.021	.046	.064	.076	.083	.086	.088	.089
	LD	raw	.023	.048	.067	.079	.086	.090	.093	.094
		sand	.023	.048	.067	.079	.086	.090	.093	.094
2	Level	raw	.006	.027	.041	.050	.055	.057	.058	.059
		sand	.006	.027	.041	.050	.055	.057	.058	.059
	LD	raw	.006	.027	.042	.051	.056	.058	.059	.060
		sand	.006	.027	.042	.050	.056	.058	.060	.060
5	Level	raw	.017	.033	.046	.054	.059	.062	.063	.063
		sand	.017	.033	.046	.054	.059	.061	.063	.063
	LD	raw	.018	.035	.048	.057	.062	.064	.066	.066
		sand	.018	.035	.048	.057	.062	.065	.066	.066
10	Level	raw	.032	.048	.061	.069	.074	.076	.077	.078
		sand	.032	.049	.061	.069	.074	.076	.078	.078
	LD	raw	.034	.052	.066	.075	.081	.085	.087	.088
		sand	.034	.052	.066	.076	.082	.086	.087	.088

Table A.16: Simulation result for LP-IV (4): Coverage probability of point-wise 90% credible interval

R	Spec.	Cov.	h							
			0	1	2	3	4	5	6	7
1	Level	raw	.889	.891	.873	.883	.886	.890	.884	.887
		sand	.888	.889	.873	.882	.886	.890	.883	.887
	LD	raw	.897	.876	.890	.885	.893	.908	.910	.915
		sand	.898	.878	.890	.886	.893	.908	.911	.914
2	Level	raw	.896	.874	.883	.867	.873	.864	.871	.879
		sand	.893	.871	.884	.867	.876	.863	.873	.879
	LD	raw	.880	.890	.894	.897	.894	.906	.899	.892
		sand	.879	.891	.898	.898	.893	.906	.900	.891
5	Level	raw	.881	.866	.839	.850	.873	.874	.862	.865
		sand	.879	.864	.845	.849	.869	.873	.865	.865
	LD	raw	.873	.869	.868	.873	.851	.856	.846	.846
		sand	.876	.870	.870	.872	.848	.858	.847	.845
10	Level	raw	.825	.809	.820	.821	.810	.808	.821	.814
		sand	.826	.812	.827	.827	.811	.809	.821	.823
	LD	raw	.826	.833	.822	.814	.818	.809	.809	.814
		sand	.826	.833	.825	.817	.818	.817	.806	.814

Table A.17: Simulation result for LP-IV (5): Coverage probability of simultaneous 90% credible band

R	Spec.	Cov.	plug-in	quantile
1	Level	raw	–	.873
		sand	.876	–
	LD	raw	–	.893
		sand	.897	–
2	Level	raw	–	.855
		sand	.854	–
	LD	raw	–	.888
		sand	.894	–
5	Level	raw	–	.810
		sand	.818	–
	LD	raw	–	.831
		sand	.844	–
10	Level	raw	–	.745
		sand	.753	–
	LD	raw	–	.758
		sand	.757	–